Russian Chemical Reviews **79** (8) 635 – 653 (2010) © 2010 Russian Academy of Sciences and Turpion Ltd

DOI 10.1070/RC2010v079n08ABEH004148

Modern diffusion-ordered NMR spectroscopy in chemistry of supramolecular systems: the scope and limitations †

S V Kharlamov, Sh K Latypov

Contents

I.	Introduction	635
II.	Methods for measurements of self-diffusion coefficients in high-resolution NMR spectroscopy: the scope and limitations	636
III.	Mathematical treatment of experimental results	644
IV.	Quantitative interpretation of self-diffusion coefficients	645
V.	Conclusion	650

Abstract. The concept of diffusion-ordered NMR spectroscopy (self-diffusion coefficients measurement in high-resolution mode) is considered. The most important aspects of interpretation of experimental data, as well as the scope and limitations of the available theoretical and phenomenological models relating the self-diffusion coefficient to the size or mass of the molecular system are discussed. The bibliography includes 219 references.

I. Introduction

Investigations of the formation of intermolecular complexes, association, self-organization, molecular recognition and rearrangements of supramolecular structures under the action of various factors belongs to the most promising avenues of modern chemical and biochemical researches. This is first of all due to the fact that such processes occur in both wildlife and inorganic nature. In biochemistry, these include metabolism and the 'bottom – up' evolution of systems from supramolecules to organs. Their occurrence in living organisms is genetically programmed and determined. In inorganic matter, there is also a rather large number of examples of how co-operative effects determine the macroscopic properties and structure. These include the catalytic effect of micellar systems, processes in organized media, *etc*. Therefore, it is very important to understand the nature of such processes, to known how one can affect the ensembles mentioned and to design novel 'smart' supramolecular systems. To reach this goal, one should reliably determine the 3D molecular structure, which is of particular importance in studies of solutions.

S V Kharlamov, Sh K Latypov A E Arbuzov Institute of Organic and Physical Chemistry, Kazan Research Centre of the Russian Academy of Sciences, ul. Arbuzova 8, 420088 Kazan, Russian Federation. Fax (7-843) 273 22 53, tel. (7-843) 272 74 84, e-mail: khsergey@iopc.ru (S V Kharlamov), lsk@iopc.ru (Sh K Latypov)

Received 2 March 2010
Uspekhi Khimii **79** (9) 699 – 719 (2010); translated by A M Raevskiy

High-resolution NMR spectroscopy proved itself as one of the most efficient experimental methods used in the research on solutions.[1 – 6] A number of efficient techniques were developed, which make it possible to determine internuclear correlations (correlation spectroscopy) and, thus, to reconstruct the topologies of molecular systems. In some cases, this permits a 'direct' determination of their structures. Internuclear correlations can be due to both direct and indirect spin – spin interactions. At present, there is almost no problems for studying systems in solutions on the level of separate molecules because NMR spectroscopy allows one to obtain comprehensive information on the spatial structure and dynamics of such systems.[6 – 17]

However, studies of the spatial structures of organized multicomponent complexes linked by weak noncovalent interactions face severe difficulties. First, problems arise due to 'indistinguishability' of signals of particular components or fragments of the system in the NMR spectra owing to spectral 'unresolvability' and, most often, 'symmetry'-driven magnetic equivalence of these components. In other words, in such cases signals of individual components in the NMR spectra are in principle indistinguishable and the number of components in the complex (associate) cannot be evaluated. Second, the potential energy surface of a multicomponent system has a very complex shape and is characterized by a vast variety of energy minima; therefore, the observed spectral and relaxation effects are averaged over different states. Eventually, conventional NMR spectroscopy techniques (analysis of the chemical shifts and nuclear Overhauser effects[18 – 20]) may appear to be inefficient.

Fortunately, in the early stage of development of NMR spectroscopy (in the 1960s) researchers found how one can estimate the parameters of molecular self-diffusion.[21] Taking account of the fact that the mobility of a system is related to its size, one can at least estimate the size of the system when other NMR parameters become noninformative. The essence of the approach is to label the spatial

† The review is devoted to the 65th anniversary of the Kazan Scientific Centre of the Russian Academy of Sciences.

positions of nuclear spins by applying a magnetic field gradient and, having repeated this operation after some time, to obtain information on molecular displacements. This allows one to assess the molecular mobility.[22–24] However, obtaining such information was for long accompanied by the loss of high spectral resolution.

Elaboration of the theory of NMR spectroscopy and improvement of experimental equipment enabled measurements of the self-diffusion coefficients (SDC) in the high-resolution mode and thus the emergence of a specific experimental method, *viz*., diffusion-ordered NMR spectroscopy (DOSY).[25–28] The possibility to relate spectral parameters to the self-diffusion coefficients makes DOSY an important experimental method suitable for separation of the spectral contributions of different components of a system under study based on different sizes of the components. Moreover, having evaluated the size of the molecular system, one can assess its packing, degree of association, *etc*.[28–33] Intuitively understandable physical sense of the correlation 'SDC–size' (the larger the molecular system the lower the SDC and *vice versa*) and simple interpretation of the DOSY spectra (no loss of spectral information) predetermined a wide practical use of this method.

At present, DOSY is a key tool of quick analysis (in some cases, the only source of information on the structure of a system under study). The technique has a great potential for the studies of ionc liquids,[34] analysis of complex mixtures[35–39] including mixtures of different isomers;[37] however, it is most widely used in studies of supramolecular systems.[31–33] First of all, these are investigations of their aggregation and self-organization,[40–53] molecular recognition[54–63] in ensembles of organic and organometallic molecules including novel catalytic systems based on transition metal complexes.[64–66] This is due to the fact that the formation of supramolecular ensembles is usually accompanied by changes in their geometric parameters, namely, an increase in the characteristic volume (mass) upon association, changes in the mobility of components of the system upon formation of inclusion complexes, *etc*. For instance, DOSY studies clearly demonstrated the formation of molecular capsules and the dependence of their stability on external conditions.[40–42] In studies of micelle formation and aggregation, the technique permits reliable detection of the formation of molecular ensembles, determination of their size, degree of aggregation, *etc*.[43–53, 64] This is a key tool for investigations of very interesting supramolecular systems called molecular machines (ensembles whose structure and behaviour can be controlled using some external factors).[51, 57, 58, 62] DOSY also has found applications in studies of biosystems,[67, 68] pharmaceuticals[69, 70] and the structure of nanoparticles.[71] Mention should be made of joint DOSY and high-resolution magic angle spinning (HR MAS) NMR studies,[72–74] which allow one to investigate diffusion in viscous and gel-like (semi-solid) samples, in particular, biological tissues,[74, 75] cells,[76, 77] lyposomes,[78] membranes,[79, 80] liquid crystals[81] and food.[82]

At the same time, DOSY studies revealed severe methodological problems due to both artifacts observed in the course of experiments and errors in numerical interpretation of the results obtained; these features cannot always be accounted correctly. To date, a number of problems have been eliminated but some of them are still to be solved, as indicated by numerous critical studies reported recently.

The authors of this review have made an attempt to generalize the available published data and their own research experience in analysis of the scope and limitations of DOSY and assessment of the sources of errors and methods of their minimization in the course of experimental design and experimental research, transformation of 'raw' experimental data to determine the SDC values, interpretation of the measured SDC to search for correlations with geometric parameters of systems under study.

II. Methods for measurements of self-diffusion coefficients in high-resolution NMR spectroscopy: the scope and limitations

Experiments on SDC measurements and various modifications of the DOSY technique have been well documented in reviews. Therefore, we will not dwell on them and only briefly outline some key issues to introduce the subject of this review; then we refer the readers to original publications (see Refs 25–33).

The simplest method of experimental determination of SDC involves the use of Hahn's pulse sequence[83] modified by Stejskal and Tanner,[21] who inserted pulsed magnetic field gradients (Fig. 1). Application of this pulse sequence to a system of nuclear spins is followed by a response (spin echo signal) whose amplitude is modulated by the SDC.

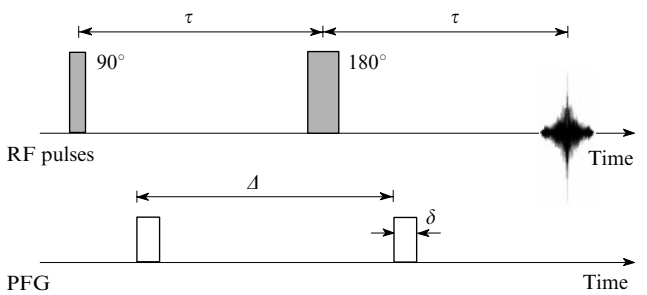


Figure 1. The Stejskal–Tanner pulse sequence.
Hereafter, grey rectangles denote the 90° and 180° RF pulses, white rectangles denote the PFG of duration δ; Δ is the diffusion time and τ is the time delay between RF pulses.

The pulsed field gradient (PFG) in the Hahn pulse sequence encodes the current spatial positon of the magnetic moment (*i.e*., the whole molecule) using its Larmor frequency. The second PFG decodes a new position at which the molecule arrives after displacement during the time interval Δ called the diffusion time. From the difference between the current value of the spin echo amplitude and its maximum value one can evaluate the displacement of the molecule from the initial position. With no temperature and concentration gradients, these molecular displacements can only be due to Brownian motion of molecules, which is characterized by the self-diffusion coefficients. Therefore, by analyzing the echo amplitude one can determine the SDC characteristic of the system in question. Practically, this is achieved by approximating the experimental dependence of the spin echo signal on the PFG amplitude by a known analytical function. This function was first obtained by Stejskal and Tanner[21] who studied free diffusion of same-type molecules in solution assuming rectangular PFG:

$$I(\delta, \Delta) = I_0 \exp\left[-D\gamma^2 g^2 \delta^2 \left(\Delta - \frac{\delta}{3}\right) - R\right], \quad (1)$$

where δ is the duration of the gradient pulse (s), Δ is the diffusion time (s), I_0 is the amplitude of the spin echo signal provided no PFG, D is the self-diffusion coefficient ($m^2\ s^{-1}$), γ is the gyromagnetic ratio ($Hz\ T^{-1}$), g is the magnetic field gradient ($T\ m^{-1}$) and R is the relaxation factor.

This dependence is called the diffusion decay and can be obtained when detecting the echo signal upon consecutive stepwise increase in the PFG amplitude.[27] The advantage of this approach is that the overal duration of the pulse sequence remains constant in the course of experiments. As a result, the relaxation and diffusion contributions can be separated with ease [see Eqn (1)]. Note that, in principle, the diffusion decay curve can also be obtained by stepwise increase in Δ or δ; however, this is not used in practice[84] because the contribution of the relaxation factor at each point will be different and analysis of experimental data will be strongly complicated.

The algorithm described above is simple in practical implementation and thus still widely used in, *e.g.*, studies of porous media.[85] At the same time, it has a severe drawback, *viz.*, analysis of the echo signal amplitudes only ‡ cannot be accompanied by simultaneous analysis of spectral data.

At first glance, it would be logical to obtain a Fourier transform of the echo signal, *i.e.*, a conventional spectrum, and to analyze the dependence of the amplitude of each signal in the spectrum on the PFG amplitude. In other words, the diffusion decay curves and, thus, the SDC would be obtained for each spectral line individually. This was practically implemented about three decades ago;[86–89] how-

‡ In studies of porous media or systems characterized by high molecular masses, it is sufficient to analyze the integrated intensity of the echo signal because, owing to physical features of these systems, their NMR spectra usually have a low resolution, *i.e.*, the recovery of spectral information from the echo signal is usually senseless.

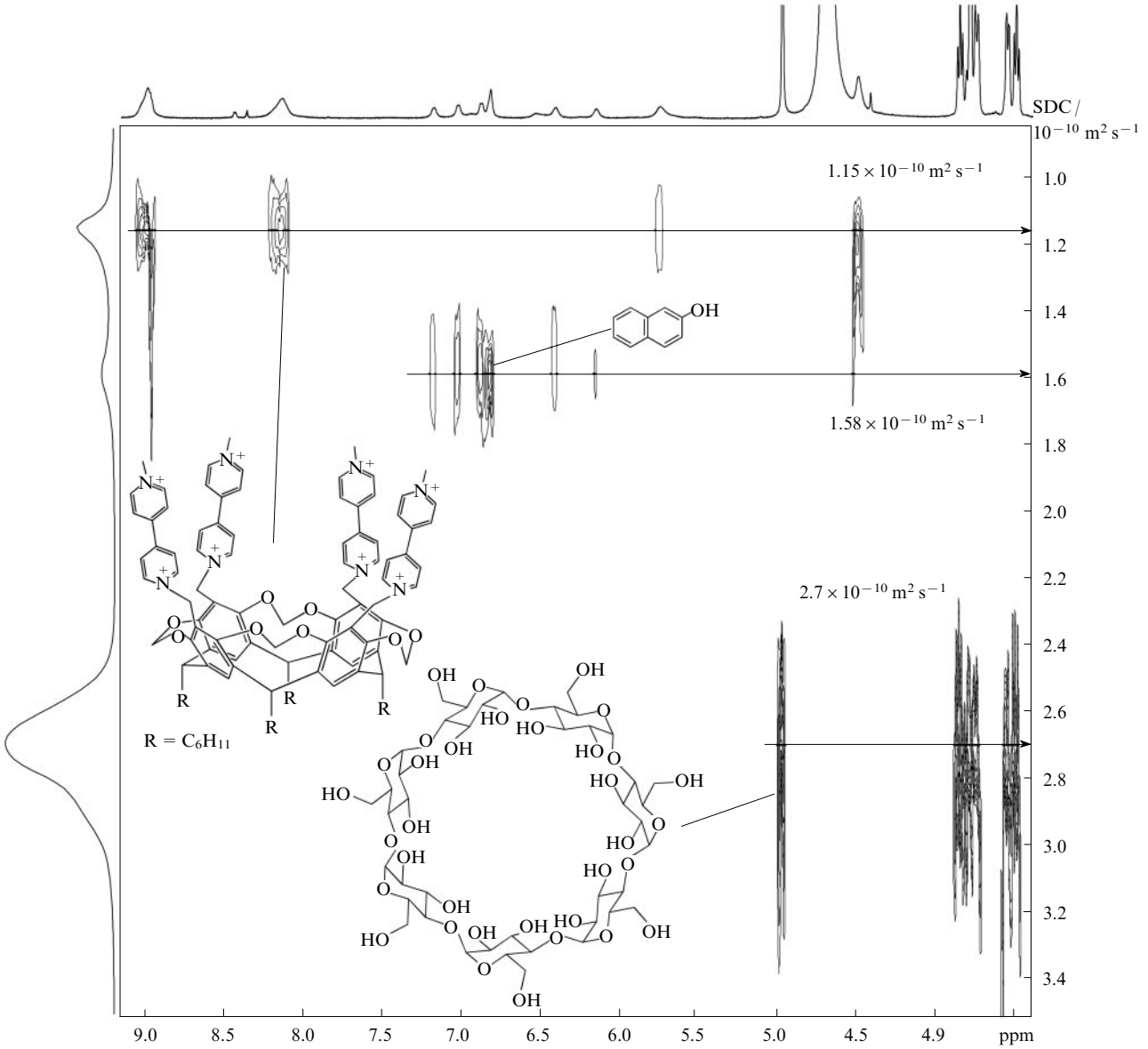


Figure 2. A DOSY NMR spectrum of a three-component system (^1H NMR, 600 MHz, 298 K, a solution in D_2O).[62]

ever, a wide use of this technique began only in the mid-1990s when a number of problems concerned with the use of PFG were solved [90] and the magnetic field gradient accessories became common parts of NMR spectrometers. First of all, the case in point is the design of systems of active-shielding of gradient coils in the NMR probes, efficient PFG generators with short swtitching times, magnetic field stabilization systems, *etc*.[26,27] The early stage of development of diffusion-ordered NMR spectroscopy also dates back to that time.[25] This allowed researchers to relate spectral (chemical shifts) information to diffusion (SDC) data (Fig. 2). If the spectra of different components are well resolved on the chemical shift scale, one can also obtain a very high resolution on the SDC scale.[29,30]

Currently, DOSY allows one to study systems with molecular masses >100 kDa (SDC $< 10^{-12}$ m^2 s^{-1}). The method is highly sensitive, permits reliable detecton of signals of compounds whose concentration can be as low as 10^{-5} mol litre^{-1}. Thus, the number of appropriate compounds and materials is very large (Table 1);[27,56,91–95] this predetermines the great need for DOSY. Moreover, since the SDC of a system under study can be assessed rapidly (within a few seconds) using specific pulse sequences, the technique can be treated as a method for quick analysis.[96–100]

Table 1. Self-diffusion coefficients of compounds measured at 298 K.

Compound	Molecular mass	SDC / 10^{-10} m^2 s^{-1}	Ref.
H_2O	18	23.0	27
D_2O	20	18.7	27
HOD in D_2O	19	19.0	27
C_6H_6 in C_6D_6	78	22.1	27
MeOH in CD_3OD	32	24.1	91
EtOH in CD_3CD_2OD	46	10.7	91
Me_2SO in $(CD_3)_2SO$	78	7.3	91
Me_2CO in $(CD_3)_2CO$	58	45.7	91
MeCN in CD_3CN	41	43.7	91
Me_4Si (1% in $CDCl_3$)	88	29.2 [a]	92
$Me_3Si(CH_2)_3SO_3Na$ (1% in D_2O)	218	6.0	93
Glucose in D_2O	180	6.8	94
Saccharose in D_2O	342	5.2	94
Raffinose in D_2O	504	4.3	94
α-Cyclodextrin in D_2O	973	3.57	56
β-Cyclodextrin in D_2O	1135	3.21	56
γ-Cyclodextrin in D_2O	1297	3.09	56
Maltodextrin in D_2O	6100	2.0	94
Poly(ethylene oxide) in D_2O	2.1×10^4	0.351	95
	1.6×10^5	0.0874	95
	5.7×10^5	0.0238	95

[a] At 300 K.

However, all experimental methods including the NMR-based determination of SDC have some limitations. Problems of DOSY experiments are first of all of hardware nature (eddy currents, quality of PFG generated, temperature gradients). They also include optimization of pulse sequences for particular samples, which in turn is determined by their properties (solvent viscosities, relaxation times of compounds under study). A large number of such problems were eliminated or minimized in the course of improvement of the technique; however, some of them are still to be solved in spite of considerable efforts.[25–32,101–105]

1. The effect of eddy currents on diffusion-ordered spectra and methods of suppression of eddy currents

Generation of PFG is accompanied by fast switching of electric current in the gradient coil and induction of eddy currents (a source of the so-called 'shaded' gradient pulses) in metallic parts of the probe around the NMR tube. Since the 'shaded' gradient pulses cannot be accounted for, this eventually leads to strong distortion of the spin echo signal. Modern probes are equipped with active-shielding systems,[27] which reduce the amplitude of eddy currents by a few orders of magnitude. However, when using large-amplitude PFG, the effect of eddy currents may be noticeable.

Methods of minimization of this effect can be divided into three groups:

— hardware solutions;
— modification of pulse sequences; and
— correction of raw experimental data.

The first group of methods includes either specific modification of the initial shape of PFG [104,106] produced by the gradient generator or dynamic shiming [107–109] to compensate the induced shaded gradients. The main practical approach involves the 'pre-emphasis' procedure [27,32,104] aimed at initial tuning of the gradient accessory of the spectrometer. The case in point is that, owing to induction of shaded gradients induced by eddy currents, the actual shape of the PFG in the gradient coil differs from the specified one (Fig. 3 *a*). During the 'pre-emphasis' procedure, parameters of the gradient generator are tuned in such a way that generation of a PFG be accompanied by some transformation of the pulse front and decay (Fig. 3 *b*). This creates conditions under which the actual shape of the PFG in the gradient coil matches the preset PFG shape. Usually, this procedure is done once and then the parameters for correction of the PFG shape are stored and used by the gradient generator without subsequent tuning. However, in each particular case the distribution of eddy currents within metallic parts of the probe can be different [105] [especially, when using large-amplitude PFG

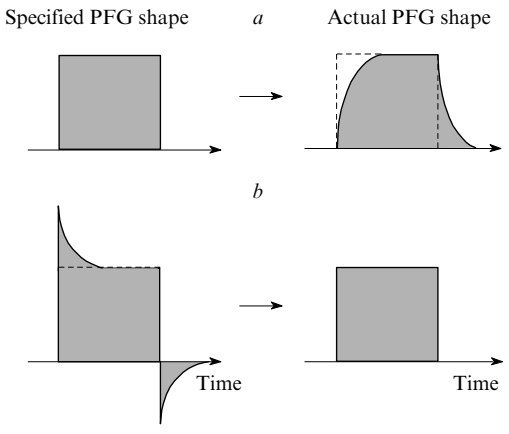


Figure 3. Illustrations of 'pre-emphasis' procedure.
The PFG shape at the input of the gradient coil and the PFG shape actually generated in the gradient coil without pre-emphasis (*a*); the same under pre-emphasis conditions (*b*).

(~ 10 T m^{-1})] and, probably, correction of parameters of the 'pre-emphasis' procedure will be required.

The second group of methods involves modificaton of pulse sequences. These methods are aimed at reducing the amplitude of eddy currents and minimizing their effect on the spin echo signal.

The first step on this way is to use non-rectangular PFG. Since the amplitude of eddy currents is proportional to the rate of the change in electric current flowing through the gradient coil,[27] the use of smoothly increasing/decreasing gradient pulses should lead to suppresion of eddy currents. For instance, the use of trapezoidal (Fig. 4 *a*) and half-sine (Fig. 4 *b*) pulses gives good results. Equation (1) can be used without modification; only the gradient g should be replaced by the amplitude of an equivalent rectangular pulse having the same area under curve (*i.e.*, δg) as the initial PFG.[110] A drawback of this approach consists in that, owing to the smaller area under curve for non-rectangular PFG compared to rectangular one at the same amplitude, the action of the former on the system will be less pronounced; this can be critically important in the studies of systems with small SDC. Moreover, even non-rectangular PFG do not allow a 100% suppression of eddy currents.

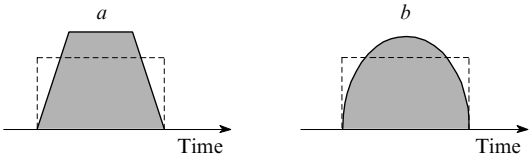


Figure 4. Different PFG shapes: trapezoidal (*a*) and half-sine (*b*). Dashed lines confine equivalent rectangular PFGs (with the same area under curve).

In this respect, pulse sequences based on the stimulated echo (STE, Fig. 5 *a*) sequences including: STE-LED (Stimulated Echo with Longitudinal Eddy current Delay, Fig. 5 *b*)[111] and especially STE-BPLED (Stimulated Echo with Bipolar Pulse pair and Longitudinal Eddy current Delay, Fig. 5 *c*) have proved themselves.[112] The STE pulse sequence offers a number of advantages[113] over the Stejskal and Tanner pule sequence (see below for detail).

Suppression of eddy currents is achieved using an additional time delay τ^* at the end of the pulse sequence. The essence is that the fourth RF pulse (see Fig. 5 *b*) causes the magnetization vector to leave the xy plane and become parallel to the z axis, thus no longer being affected by the shaded gradients induced by eddy currents. The magnetization vector retains its orientation over the time interval τ^* (usually, a few milliseconds), which is long enough for eddy currents to decay.[29] Then, under the action of the last RF pulse in the pulse sequence the magnetization vector again goes to the xy plane, which is followed by detection of the echo signal.

The STE-BPLED pulse sequence (see Fig. 5 *c*) differs from STE-LED in that it uses composite gradient pulses (two PFG having halved duration and opposite signs separated by a 180 RF pulse) instead of single PFG. Since the gradient pulses have opposite signs, eddy currents induced by them are partially cancelled.[114, 115] Moreover, composite PFG offer additional advantages, *e.g.*, they allow

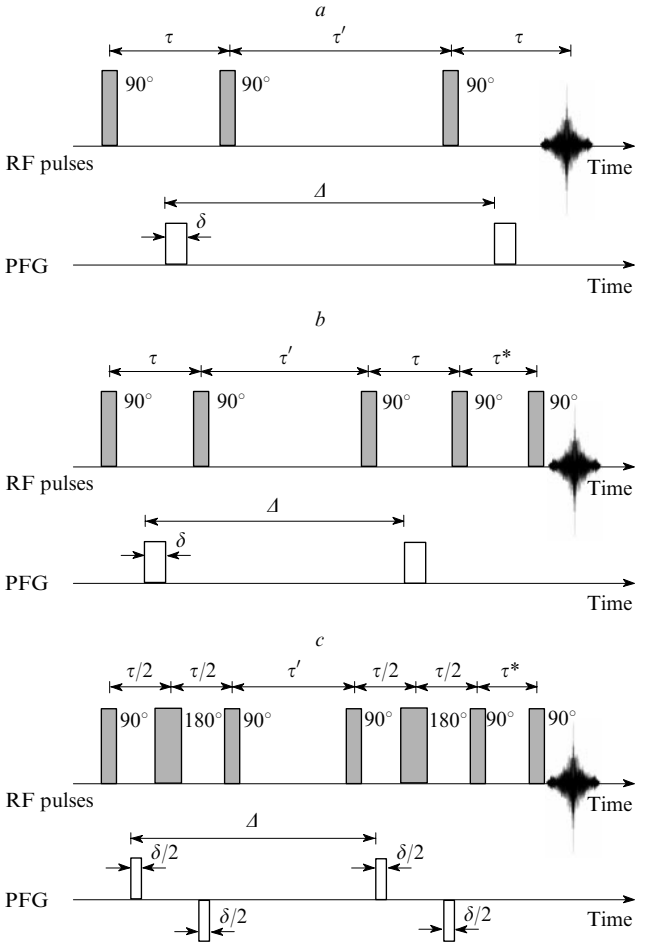


Figure 5. The pulse sequences: STE (*a*), STE-LED (*b*) and STE-BPLED (*c*);
τ, τ' are the time delays between RF pulses and τ^* is the time delay for suppression of eddy currents.

one to minimize the effects of inhomogeneity of the main magnetic field B_0 and cross-relaxation (see below).[113]

The third group includes methods involving specific kinds of mathematical treatment of free induction decays.[27, 101, 102] In this case, the key problem is to minimize spectral distortions caused by eddy currents rather than to suppress eddy currents. However, such methods are of limited use.

2. Effect of PFG quality on measurements of self-diffusion coefficients

Practically, gradient pulses generated in a gradient coil can be considered uniform only in the central part of the coil.[27, 29] Moreover, it is not known with certainty that the gradient pulse generated in the coil is identical to that produced by the gradient generator. As a result, the PFG amplitude in that part of the sample that is excited by the RF coil can vary within 30%. At the same time, any deviation from the preset PFG shape or amplitude leads to distortion of the character of the diffusion decay. Eventually, the SDC determined in different regions of the same sample can vary within 50%. A small systematic error is admissible when comparing the relative values of SDC but inadmissible when carrying out quantitative measurements.

A number of methods for solving these problems were proposed.[27, 29, 103, 116–133] The most appropriate algorithms proved efficient are considered below.

Generally, a method for excitation of a sample with PFG having specified parameters includes two interrelated steps. Therefore, optimization of PFG may require a number of iterations.

Step 1. Determination of PFG amplitude. The absolute value of the magnetic field gradient produced in a gradient coil is proportional to the electric current flowing through the coil. The coefficient of proportionality (calibration constant) g_{cal} is a unique characteristic of a particular probe. Therefore, prior to going to diffusion measurements, one should accurately determine this parameter.

Theoretically, the g_{cal} value and even the PFG shape can be calculated in each case from the known geometric parameters, the number of turns in the coil and the electric current flowing through the coil. However, if the gradient coil is surrounded by certain metallic parts (even if the active shielding system is available), accurate calculations are impossible. Therefore, this method is used only in the first step of operation with a noncalibrated gradient coil to estimate the amplitude of a PFG produced at a specified electric current flowing through the coil.

To allow for all features of the gradient pulse actually produced within the sample, one should carry out test experiments using a sample with the known SDC. However, one should take into account the fact that the nonlinearity of the PFG, eddy currents, *etc*. depends on the electric current flowing through the gradient coil. Therefore, the described algorithm is most efficient when measurements with an actual sample are carried out under identical conditions including the same time delays and the pulse durations and amplitudes as those used in the pulse sequence. Thus, exact determination of the SDC of a system under study requires preliminary experiments with a reference sample having a similar SDC under identical conditions. For systems with relatively high SDC, the choice of appropriate references is not a problem;[90, 94, 120–126] otherwise, it becomes problematic.[127]

Step 2. Taking account of the spatial profile of a PFG. All conclusions about correlations between the SDC and the shape of the diffusion decay curve (see above) were drawn assuming that the magnetic field gradient produced in a sample has a particular constant value in the bulk of the sample. At the same time, almost all available types of gradient coils provide no possibilities of producing such PFG.[27, 29] A perfect, almost ideal magnetic field homogeneity can be achieved only in the so-called HR MAS probes equipped with a Z-axis gradient coil.[134] However, such probes for liquid samples are rare[134] because, on the one hand, HR MAS probes are not integral parts of conventional 'liquid-phase' NMR spectrometers and, on the other hand, operation with the HR MAS probes has some specific features.

In conventional high-resolution NMR probes equipped with a gradient coil, the PFG homogeneity region is usually limited to a distance of about 10 mm near the centre of the gradient coil. Therefore, the shape of the experimentally observed diffusion decay will differ from the ideal shape[118] [see Eqn (1)]. For instance, the SDC of water[29] ($T = 296$ K) determined using the first five points in the diffusion decay curve (small PFG amplitude) is 1.79×10^{-9} m^2 s^{-1} (*cf*. 1.60×10^{-9} m^2 s^{-1} obtained using the last five points in the diffusion decay curve, where the PFG amplitude approaches a maximum value). Calculations using all points in the diffusion decay curve give a value of 1.71×10^{-9} m^2 s^{-1}. Thus, the SDC value is determined with a large error, which increases as the PFG amplitude increases.

a. Physical reduction of sample height

There are a number of methods for producing spatially constant-amplitude PFG in a sample. One of them is to reduce the height of the sample under study to the size of the PFG homogeneity region.[29, 133] At the same time, this can lead to the loss of homogeneity of the magnetic field B_0 in the bulk of the sample. As a result, the use of samples shorter than 30 mm appears to be unreasonable.[133]

To avoid strong distortion of the magnetic field at sample boundaries, it is appropriate to use a short sample placed between two inserts with properly matched magnetic susceptibility and with the required total height. Such inserts may be made from solid materials with special composition[128, 129, 135] or liquids producing no signals at the frequency of the nuclei under study.[27] However, this technique is of limited use because of difficulties in choosing appropriate inserts with the necessary magnetic susceptibility for arbitrary samples.

b. Modification of pulse sequence

A good approach aimed at minimizing the PFG nonlinearity is to modify the pulse sequence. As a result, the signal is received only from that fragment of the sample where the PFG gradient has a maximum homogeneity. This is achieved by excitation of a small fragment of the sample at the centre of the gradient coil.

An example is provided by the 'Slice-Selection' technique[29, 130] whose idea was taken from NMR imaging.[136] Namely, the action of a 90° pulse which excites a desired frequency region (about 10 kHz for ^{1}H nuclei) is accompanied by application of a small-amplitude gradient. As a consequence, the resonance conditions are met only within the small spatial region at the centre of the sample where the additional magnetic field produced by the gradient coil is nearly zero. By varying the gradient one can choose slices as thin as necessary but thick enough to avoid the influence of the molecules penetrating the active layer during the acquisition time on the diffusion decay. This condition is met if the layer is a few millimetres thick.[29] For instance, the self-diffusion coefficients of water (nearly 3-mm thick layer) determined using the first five, last five and all points in the diffusion decay curve are almost equal (2.25×10^{-9}, 2.23×10^{-9} and 2.22×10^{-9} m^2 s^{-1}, respectively) and close to the actual SDC of water molecules.[29]

Yet another method is to augment the pulse sequence with a specific adiabatic inversion pulse,[131, 132] which also excites only the central fragment of the sample.

In spite of attractive features of these approaches, they are of limited use because selection of a slice in the sample unavoidably reduces the signal-to-noise ratio.

c. Parameterization of Stejskal–Tanner equation with allowance for PFG shape

At present, the most efficient method of solving problems concerned with a nonideal PFG shape involves calculations of the deviation of the actual PFG shape from a perfect one.[103, 116, 119] The case in point is that application of a real PFG whose amplitude varies along the sample leads to multiexponential diffusion decay even for one-component

molecular systems. It was proposed to quantitatively describe the actual shape of the gradient pulse and then to modify the Stejskal–Tanner equation (1) in appropriate manner.

The Stejskal–Tanner equation can be modified in two ways. One of them is called a 'direct' procedure and based on representation of the diffusion decay by a function of the squared nominal amplitude of the gradient pulse for a sample with the known SDC. The diffusion decay thus obtained is then approximated by an appropriate function (distribution function,[103] exponential of a power series [119]) with corresponding variables to take into account the observed deviation of the experimental curve from that described by Eqn. (1).

A modified Stejskal–Tanner equation has the form:[103]

$$I(\delta, \Delta) = I_0 \frac{\int \rho(g_{cal}) \exp\left[- D\gamma^2 (I g_{cal})^2 \delta^2 (\Delta - \delta/3) \right] dg_{cal}}{\int \rho(g_{cal}) dg_{cal}}. \quad (2)$$

Here, the amplitude g of the gradient pulse was replaced by Ig_{cal} taking account of its proportionality to the electric current I flowing through the gradient coil. At the same time, the g_{cal} value varies along the sample from g_{cal}^{min} to g_{cal}^{max} when PFG applies (see above); therefore, the observed spin echo decay at a specified electric current I should be weighted with the weight function $\rho(g_{cal})$. The boundary condition is as follows: the function $\rho(g_{cal})$ should be zero outside the active region of the sample.

The function $\rho(g_{cal})$ can be determined upon carrying out the Stejskal–Tanner experiment with a weak magnetic field gradient applied during the signal acquisition time. As a result, one gets an image of the sample (as in NMR imaging).[29, 103] Would the PFG be linear within the whole excited volume of the sample, this experiment should result in a rectangular spectrum (Fig. 6 *a*). The actual spectral shape is more complicated because it characterizes the $\rho(g_{cal})$ distribution (Fig. 6 *b*).

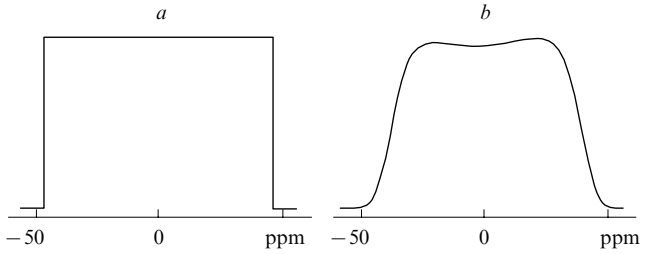


Figure 6. The expected (*a*) and actual (*b*) 1D images of the sample (^{1}H NMR, 400 MHz, 298 K, 10% D_2O–90% H_2O).

At the same time, an analysis of the series of 1D profiles for a model sample with a known SDC obtained upon successive increase in the electric current in the gradient coil makes it possible to determine the form of the function $\rho(g_{cal})$.[103] Taking into account the fact that in conventional probes the amplitude distribution of the magnetic field gradient along the sample is rather narrow (usually, the PFG at the periphery is about 25% weaker than at the centre of the gradient coil [27, 29, 103]), the g_{cal} distribution is correctly described as follows:

$$\rho(g_{cal}) = \begin{cases} 0, & g_{cal}^{min} > g_{cal} > g_{cal}^{max} \\ \dfrac{2(g_{cal} - g_{cal}^{min})}{(g_{cal}^{max} - g_{cal}^{min})^2}, & g_{cal}^{min} < g_{cal} < g_{cal}^{max} \end{cases}.$$

This distribution was obtained for a reference sample (1% H_2O in $D_2O + 10^{-3}$ kg litre^{-1} $GdCl_3$), and can then be used for all samples as a characteristic parameter of the probe chosen.[103]

Eventually, Eqn (2) with the found distribution parameters takes the form

$$I(\delta, \Delta) = \frac{2}{\left(g_{cal}^{max} - g_{cal}^{min}\right)^2} \left\{ \frac{\exp\left(-q g_{cal}^{min^2}\right)}{2q} - \frac{\exp\left(-q g_{cal}^{max^2}\right)}{2q} - \right.$$
$$\left. - \frac{\pi^{1/2} g_{cal}^{min}}{2q^{1/2}} \left[\mathrm{erf}\left(q^{1/2} g_{cal}^{max}\right) - \mathrm{erf}\left(q^{1/2} g_{cal}^{min}\right) \right] \right\},$$

where

$$q = \gamma^2 I^2 \delta^2 D \left(\Delta - \frac{\delta}{3}\right),$$

$$\mathrm{erf}(z) = \frac{2}{\pi^{1/2}} \int_0^z \exp\left(-t^2\right) dt.$$

When using this modification of the Stejskal–Tanner equation, the root-mean-square error in the approximation of the diffusion decay decreases by more than an order of magnitude compared to the case where nonlinear character of PFG is ignored.[103]

However, it should be noted that the 'direct' technique requires a great care. The point is that in the experiments with a reference sample to obtain the parameters of the modified Eqn (2) one has to exclude the effects of all other factors apart from nonlinearity of the PFG, but also (temperature gradients, undesired coherence transfer channels, *etc.*) on the SDC value to be measured.

The 'indirect' technique [119] is free from these drawbacks because it assumes mapping of the spatial distribution of the signal and the profile of the gradient pulse for a particular sample. Then one should calculate the expected form of the dependence of the diffusion decay for the entire sample and approximate it as in the 'direct' method. This technique is more general because it assumes inhomogeneity of the RF field in the bulk of the sample; this is ignored by other approaches.

In this case, the Stejskal–Tanner equation (1) should be modified as follows:[116, 119]

$$I(\delta, \Delta) = I_0 \exp\left(- \sum_{n=1}^{N} c_n \hat{q}^n g_{cal}^{2n} I^{2n} \right),$$

where c_n are the weighting coefficients which characterize the degree of deviation of the actual diffusion decay on the monoexponential curve (coefficient c_1 has a clear physical meaning, namely, it characterizes the deviation of the sample-averaged actual gradient value from the nominal one);

$$\hat{q} = \gamma^2 \delta^2 D \left(\Delta - \frac{\delta}{3}\right).$$

This model can also be used for highly nonlinear PFG.[119]

An advantage of these approaches over the 'Slice-Selection' method is that the signal-to-noise ratio is retained because these techniques 'operate' with the whole sample volume excited by the RF coil. However, experiments based on mapping of the spatial profiles of the gradient and RF pulses require enhanced phase cycling and, therefore, a much longer time and the use of much more complicated pulse sequences.

Thus, production of a PFG with preset parameters (amplitude, shape, homogeneity) within the sample under study is a multistep process. First, in the case of non-calibrated gradient coil one should calculate parameters of the PFG to be created at a specified electric current flowing through the coil. For commercially available equipment, this step is usually to a good accuracy performed by the manufacturer. Second, one should map the 3D profile of the gradient pulse to obtain information on the deviations of the actual PFG parameters from the expected values. The employed mathematical algorithm of processing of experimental data should be modified taking into account these deviations. Eventually, if possble, having chosen a reference sample (depending on the type of the system under study) with the known SDC value, one should ensure that the previous steps were done efficiently, *i.e.*, the SDC to be measured should be equal to the known value (obtained by some alternative method). Having done this, one can be assured that the error introduced into the measured SDC values by the 'nonideal' PFG shape is minimum.

3. Temperature gradients within the sample and how to reduce them

Convective flows in a sample represent yet another factor which can introduce large errors in the SDC determination. Since the temperature of the sample placed into the probe of an NMR spectrometer is stabilized by a gas flow having a specified temperature, which blows the tube from the bottom, the sample is heated nonuniformly, which creates a temperature gradient. If this gradient is rather large, longitudinal convective flows of the liquid along the sample appear which are superimposed with diffusion flows. This causes strong distortions of the diffusion decays (up to sinusoidal modulations of the decay curve). Despite the fact that this source of errors in the determination of SDC has been a subject of scientific discussion,[137–139] the problem of efficient elimination of temperature gradients or at least correct allowance for these effects when analyzing the results obtained is still to be solved.[135, 139, 140]

There is a number of methods for minimization of temperature gradients in the sample. First of all, this is the use of high-quality temperature stabilization system because the SDC depends on temperature very strongly. In most cases it can be approximated by the expression derived within the framework of the Frenkel activation model: [84, 141]

$$D = D_0 \exp\left(-\frac{E_d}{RT}\right),$$

where

$$D_0 = \frac{\delta^2}{6\tau_0}$$

is the temperature-independent factor in which δ is the length of an elementary jump of the molecule from one equilibrium position to another (m), τ is the period of molecular oscillations near the equilibrium position (s); E_d is the activation energy of self-diffusion (J), R is the universal gas constant (J mol^{-1} K^{-1}) and T is absolute temperature (K).

This leads to a situation when the SDC varies by a few per cent as the temperature changes by a degree; therefore, any instability of the temperature regime can lead to noticeable errors.

Yet another important method for attainment of uniform temperature distribution within the bulk of the sample involves the use of intense gas flow, especially at temperatures different from ambient one.[133, 137] Unfortunately, at higher temperatures very intense gas flows are needed (> 1 m^3 h^{-1}) and this approach can lead to errors associated with tube vibrations, *viz.*, vibration-induced motions of the sample can superimpose with the diffusion motion and thus cause significant distortions of experimental results. Similar problems can also arise when cooling with nitrogen flow in the course of low-temperature experiments.

An alternative (or an additional) method is to physically reduce the sample volume (diameter and/or height).[27, 29, 130, 137] First of all, it is recommended to reduce the diameter [142] because longitudinal flows are minimized owing to friction on tube walls. At the same time, reduction of the sample volume unavoidably leads to a decrease in the signal-to-noise ratio and even to the loss of the magnetic field homogeneity (especially, at the boundaries) if the sample volume is reduced considerably. Eventually, this can cause a large broadening of spectral lines and complication of analysis of the results obtained. To solve this problem, one can use specially shaped tubes [135] in which the volume of the sample is confined from both sides by two inserts whose magnetic susceptibility is chosen to be close to that of the solution.[129, 135] At the same time, this technique is expensive and inconvenient because the material of the inserts should in fact be chosen for each sample.

All methods described above may appear to be insufficient to minimize the effects of convection if samples are of low viscosity. In this case, it is useful to use modified pulse sequences which minimize the effects of mass transfer in the sample.[143–145] For instance, with the double stimulated echo (DSTE) pulse sequence [143, 144] (Fig. 7) the effective temperature gradient in the sample becomes equal to zero because the phase shift produsd by the mass flow at a constant rate is zero (laminar flow). Examples of correct

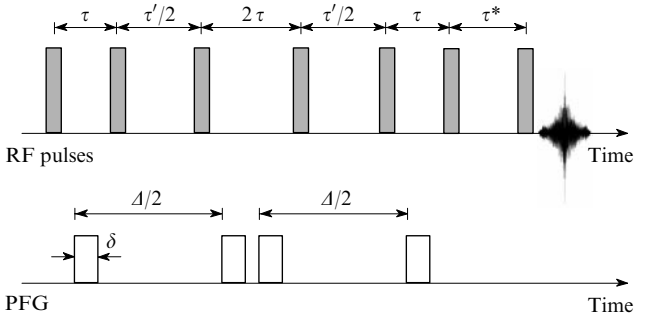


Figure 7. The double stimulated echo pulse sequence for compensation of convective flow effects with a time delay for suppression of eddy currents.

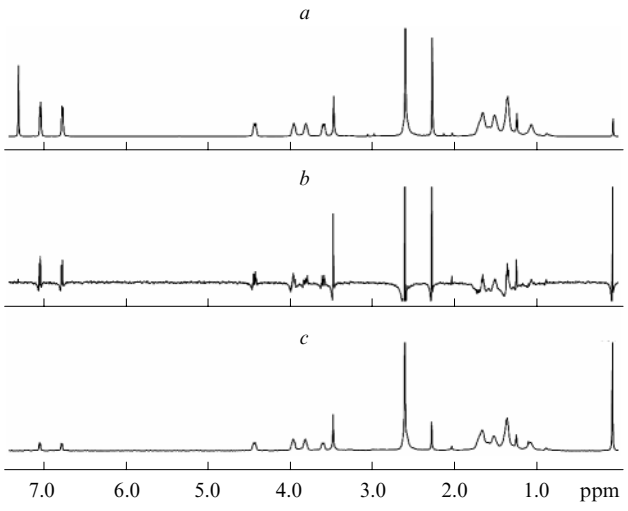


Figure 8. NMR spectra obtained using the STE-BPLED (*a*, *b*) and DSTE (*c*) pulse sequences.
PFG amplitude: 2% (*a*) and 95% (*b*, *c*); ^{1}H NMR spectrum (600 MHz, 253 K, in $CDCl_3$ solution).

determination of SDC values using this pulse sequence even at a relatively high temperature (347 K) were reported; the error in SDC determination was one tenth of that obtained with the STE-BPLED pulse sequence.[143, 144]

The DSTE pulse sequence is highly efficient in low-temperature experiments, in which production of intense uniform flows of the cooling gas is difficult and the use of tubes with a smaller diameter is undesired owing to a decrease in the signal-to-noise ratio. A comparison of the results obtained after application of one-dimensional STE-BPLED and DSTE pulse sequences to the sample under study ($CDCl_3$ as solvent, $T = 253$ K) using the PFG with an amplitude of 95% of its maximum value (Fig. 8) clearly demonstrates the effect of convection and significant phase distortions of the signals. As a consequence, the error in the determination of SDC appears to be very large. At the same time, the spectrum obtained with the DSTE pulse sequence is undistorted§ and the SDC can be determined with a good accuracy (error $< 10\%$).

A drawback of the DSTE pulse sequence is the need for enhanced phase cycling. In addition, the overall sensitivity of this pulse sequence is somewhat lower than that of, *e.g.*, STE-BPLED sequence because of the longer duration of the DSTE sequence. As a result, the corresponding relaxation decay is also longer.[143] However, it is clear that in some cases the loss of sensitivity can be compensated by the gain from minimization of convection.

Thus, neglect of temperature gradients can have a dramatic effect on the results of diffusion experiments. To eliminate the problem, one should stabilize the temperature of the sample. To this end, it is desired to carry out measurements at temperatures near room temperature using high intensities of gas flows to blow the sample. If this is insufficient or impossible, one can reduce the diameter/height of the sample and/or use specific pulse sequences.

§ The reference spectra recorded at a PFG intensity of 2% of the maximum amplitude using both pulse sequences are similar (see Fig. 8 *a*).

4. Specific properties of samples

a. Short relaxation times

In some cases, SDC measurements can be precluded by 'inconvenient' (short) relaxation times of compounds. Since most pulse sequences used for the determination of SDC are relatively long, fast relaxation can cause a strong decrease in the amplitude of the echo signal at the end of the sequence. This problem is of particular importance in experiments with supramolecular systems, proteins and when the spin labels used are not protons.

In principle, from Eqn (1) it follows that shortening of relaxation times does not introduce errors when determining the SDC value. One should only observe a decrease in the amplitude of the spin echo signal. However, in some cases this precludes full-scale experiments owing to small signal-to-noise ratio, especially at large PFG amplitudes. Moreover, shortening of the spin–spin relaxation time leads to broadening of resonance lines, which can strongly complicate processing of experimental results.

There is a number of approaches to eliminate this problem. For instance, the transverse relaxation time can be increased using the spin decoupling technique[3] or MAS with Z-axis gradient coils.[81, 146] However, both methods require specific conditions (for the second method, in particular, a tailor-made gradient probe is needed); therefore, they are of limited use.

At the same time, taking into account the fact that the spin–lattice relaxation time (T_1) is often longer than the spin–spin relaxation time (T_2), it is appropriate to apply the RF sequences in which the magnetization vector during the longest time interval Δ is aligned to the z axis rather than lies in the xy plane of the rotating frame where the spin–spin relaxation 'operates' (in this case, the relaxation rate is $R \sim 1/T_2$). In the former case, one has $R \sim 1/T_1$, *i.e.*, the relaxation contribution in Eqn (1) may appear to be much smaller.

The simplest example illustrating the aforesaid is provided by the STE pulse sequence (see Fig. 5 *a*)[147] in which the second RF pulse is applied immediately after the first PFG in contrast to the Stejskal–Tanner pulse sequence (see Fig. 1). Since this is a 90° pulse, it flips the magnetization vector along the z axis, where this vector spends the time τ, *i.e.*, the longest part of the diffusion time Δ. This offers a number of advantages. First, the effect of eddy currents is minimum because the shaded gradients induced by them are usually aligned to the z axis and have in this direction the most pronounced effect on the precession of the magnetic moments in the xy plane. Second, the effects of J-modulation, which may occur in systems with strong spin–spin interaction, are minimized.[27] Eventually, when the magnetization vector is parallel to the z axis, the defocusing gradients can be applied to the system; they affect the residual magnetization in the xy plane (the residual magnetization can be due to, *e.g.*, nonideal shape of the RF pulses). This leads to great improvement of the final spectra. At the same time, this pulse sequence has a significant drawback (see also Section II.4.b), *viz.*, the amplitude of the detected echo signal is halved compared to that obtained using the Stejskal–Tanner pulse sequence. This is due to the fact that the second 90° pulse (see Fig. 5 *a*) flips only 50% of the total number of magnetic moments (x- or y-component).

Nevertheless, the advantages of this pulse sequence usually compensate its drawbacks. Therefore, at present the most widely used pulse sequences are based on the STE sequence.

To avoid the problems concerned with relaxation, it seems logical to reduce, to the maximum possible extent, the durations of all time intervals between RF pulses. First of all, the point is the diffusion time Δ. However, it cannot be shortened arbitrarily because the condition $\Delta > \delta/3$ [see Eqn (1)] should be met. Therefore, this shortening may appear to be insufficient for systems with low SDC (for which δ should be large).

In this situation, one could use large-amplitude PFG (the larger the PFG amplitude the shorter the duration of the pulse sequence). Modern commercially available high-gradient diffusion probes allow one to produce PFG > 20 T m^{-1}. However, this is accompanied by more pronounced effects of various negative factors, first of all, eddy currents, and obtaining high-resolution spectra under the SDC measurement conditions seems to be problematic.

The design of most conventional high-resolution probes equipped with gradient coils enables reliable operation with PFG of the order of 0.5 T m^{-1}. Successful examples of production of higher PFG in this type of probes are scarce.[127,148] For instance, the signal-to-noise ratio in the DOSY spectra obtained in a ^{31}P NMR study of phosphoramidate ligand at 235 K (T_1 = 360 ms, T_2 = 33.9 ms) using a PFG of about 1.5 T m^{-1} was about 40% larger than in the corresponding spectra recorded at a conventional PFG of 0.5 T m^{-1} (Ref. 148). The SDC values measured appeared to be undistorted.

Practical implementation of this approach requires taking account of the fact that high PFG also induce noticeable mechanical strain in the gradient coil. Therefore, first of all one should choose an optimum power for a particular probe design. The next key step includes a stepwise calibration of the gradient produced (see Section II), which also has some features.[127] Taken altogether, this undoubtedly makes the approach in question of limited use.

At the same time, if the ^{1}H relaxation times are short, an alternative may be provided by operation with some another nucleus (^{13}C, ^{15}N, ^{31}P, *etc.*) characterized by a longer relaxation time.[149–151] Unfortunately, small gyromagnetic ratios and low natural abundance of isotopes of nuclei with appropriate characteristics usually cancel out the gain in the signal-to-noise ratio obtained owing to the longer relaxation time.

Yet another elegant technique, which may be useful in studies of systems with short relaxation times, is to use the singlet state[152,153] for which the characteristic relaxation time is usually much longer than T_1. One can create a singlet state in a two-spin system coupled by a scalar interaction.[152] Excitation of the zero-quantum transition may give rise to a mixed singlet-triplet state. The singlet and triplet components have the characteristic relaxation times T_1 and T_s, respectively ($T_s \gg T_1$). This makes it possible to create a two-spin ensemble, which is almost isolated from the environment and relaxes very slowly. For instance, 2-chloroacrylonnitrile is characterized by T_1 of about 5 s and $T_s \approx 43$ s at 298 K. At 227 K, one has $T_1 < 1$ s, which is inconvenient for operation, whereas $T_s \approx 8$ s, and one can reliably determine the SDC value for this compound.[153]

Thus, to avoid strong relaxation decays when recording the diffusion decays, it is appropriate to use the pulse sequences based on the STE sequence with the shortest possible diffusion time. If this is insufficient, stronger PFG can be applied or the nuclei with longer relaxation times used. Methods based on creation of the singlet state may also appear to be useful. However, this requires much more complicated pulse sequences characterized by long-term tuning. Thus, at present there are no universal algorithms of the SDC determination in the systems with very short relaxation times.

b. Effect of spin diffusion and cross-relaxation on the stimulated echo signal

Unfortunately, the STE-based pulse sequences are not free from certain drawbacks.

First, if the magnetization vector is aligned to the z axis (this occurs when using the STE pulse sequence), spin diffusion may appear (in, *e.g.*, studies of macromolecules).[113] This manifests itself as a greater decrease in the echo amplitude with the increase in Δ compared with the values expected from the relaxation times for a given system. This problem can be eliminated by including composite gradient pulses comprising two PFG with opposite signs[113–115] (see Fig. 5 *c*) instead of single PFG in the pulse sequence.

Second, problems in the experiments with the STE pulse sequence may also appear due to the cross-relaxation effect.[113,154–156] Intramolecular cross-relaxation leads to distortion of the shape of the signals of the nuclei coupled by the spin–spin interaction (AB-systems) and the degree of distortion increases with an increase in Δ. In this case, the use of composite PFG also eliminates the problem.[113,155] At the same time, the efficiency of composite PFG may decrease in the presence of intermolecular cross-relaxation (the measured SDC depends on Δ).[154,156] Nevertheless, in some cases the SDC can be determined exactly.[154] Moreover, experiments with some other nucleus may be useful provided no cross-relaxation for that nucleus.[156]

Thus, it is appropriate to use bipolar composite PFG instead of single gradient pulses when applying the STE-based pulse sequences. One should also ensure that no intermolecular cross-relaxation occurs in the system under study.

III. Mathematical treatment of experimental results

The problem of correct mathematical treatment of experimental results including the case of polydisperse systems has been well documented.[28,29,30,157–176] There is a large number of suitable algorithms. We will briefly outline only some key issues.

Remind that the Stejskal–Tanner experiments give a set of spin echo signals (only the second half of the echo signal is used for analysis[26,27]) whose amplitudes successively decrease according to Eqn (1). In other words, this is a two-dimensional matrix of amplitudes $\tilde{E}(g,t)$, where g is the magnetic field gradient and t is time. To obtain a DOSY NMR spectrum, this matrix is transformed twice. First, the Fourier transformation $\tilde{E}(g,t) \Rightarrow E(g,\nu)$ is performed. The matrix $E(g,\nu)$ (ν is frequency) represents a set of one-dimensional spectra in which the amplitudes of the resonance signals decrease with an increase in g. The final step includes passage from $E(g,\nu)$ to the DOSY NMR spectrum, *i.e.*, to the matrix $S(D,\nu)$, where D is the SDC. There is a large number of algorithms suitable for performing the transfomation $E(g,\nu) \Rightarrow S(D,\nu)$.

From Eqn (1) it follows that if a system contains n components and each of them is characterized by its own SDC (D_n), the expression for $E(g,\nu)$ can be written in the form

$$E(g,v) = \sum_n A_n(v) \exp\left[-D_n\gamma^2 g^2 \delta^2 \left(\Delta - \frac{\delta}{3}\right)\right], \quad (3)$$

where $A_n(v)$ is the spectrum of the nth component (with allowance for the relaxation factor).

The transformation $E(g,v) \Rightarrow S(D,v)$ is based on stepwise analysis of the diffusion decays obtained at each frequency point (or for a small number of successively arranged frequency points called a frequency channel). Then, depending on the properties of the system, one can choose a particular algorithm of this transformation.

1. The Levenberg – Marquardt method

If all signals along the chemical shift axis are resolved and the system is characterized by a discrete set of SDC values, the diffusion decays obtained for each frequency channel can be approximated with ease by the function (1) using a conventional Levenberg – Marquardt statistical method¶ (least squares method).[158, 159] This requires knowledge of the starting SDC values that are optimized in the course of approximations. The main advantages of this method are its unambiguous character and simplicity.

In the absence of spectral overlap, it is sufficient to use the algorithm described above. However, this is a rare case for real systems and eventually, the method becomes inefficient.[29] This gave an impetus to the development of some techniques of different complexity, which to one extent or another allow one to solve the problems concerned with the overlap of individual spectral lines.

2. The DISCRETE method

The DISCRETE (Discrete Sum of Exponential Decays) method[25, 160, 161] provides an alternative to the Levenberg – Marquardt method. It does not require the set of starting SDC values; this is convenient when there is little information on the system. At the same time, a drawback of this approach consists in that the SDC values obtained for a number of frequency points within the same signal of a particular compound often significantly differ from one another.

3. The SPLMOD method

The SPLMOD (Spline Model) method[162, 163] represents a logical development of the DISCRETE approach. It also does not require the set of starting SDC values; however, in operation with several frequency channels within a single line all channels are analyzed simultaneously. The solution is admittedly found within the standard deviation near the SDC value to be determined. The input data for the SPLMOD algorithm should be pre-treated in some way,[28] which in some cases is difficult to do.

4. The CONTIN method

Polymers or vesicles often exhibit continuous molecular mass distributions and, therefore, continuous SDC distributions. This requires modification of expression (3):

$$E(g,v) = \int_0^\infty a(D,v) \exp\left[-D_n\gamma^2 g^2 \delta^2 \left(\Delta - \frac{\delta}{3}\right)\right] \mathrm{d}D\,,$$

where $a(D,v)$ is the one-dimensional spectrum of the system at a specified SDC value.

The CONTIN (Continuous Distributions of Exponentials) method[164–166] uses the constrained regularization algorithm for correct transformation $E(g,v) \Rightarrow S(D,v)$. This algorithm can lead to physically incorrect solutions (negative SDC). However, if the boundary conditions are specified appropriately, the algorithm allows the SDC to be determined with a reasonable accuracy. A feature of the CONTIN method is that the peaks along the SDC axis are smoothed and therefore broadened even for monodisperse samples. However, taking into account the fact that usually in studies of most polydisperse systems the contributions of monodisperse components can be determined with ease, this feature is not a serious drawback.[167]

5. The MaxEnt method

The MaxEnt (Maximum Entropy) method[168, 169] is based on the idea of determination of the 'most probable' SDC spectrum $S(D,v)$ by maximization of the entropy of the spectral distribution under particular boundary conditions. In some cases, this approach gives more accurate results than all other techniques.[168] It does not require a complex adjustment or pretreatment of data.

6. The DECRA method

In the previous Sections, we considered the methods involving simultaneous analysis of only one or a few frequency channels using a part of available spectral information. Starting with the DECRA (Direct Exponential Curve Resolution Algorithm) method,[170–172] a number of algorithms were elaborated, which are based on simultaneous analysis of all frequency channels. Eventually, this allowed the problem of spectral overlap to be solved. The DECRA approach† does not require *a priori* information on the sample and allows one to obtain undistorted spectra of system's components with different SDC.[172, 173]

7. The MCR and CORE methods

The MCR (Multivariate Curve Resolution) method[174] is an alernative to the DECRA method and generally gives the same quality results. The CORE (Component Resolved NMR) method[174, 175] is a general two-level least squares algorithm, which allows one to perform the transformation $E(g,v) \Rightarrow S(D,v)$ using a pre-selected model. The method does not require the set of starting SDC values.

Summing up, it should be noted that none of many available methods for the determination of SDC values from the results of the Stejskal – Tanner experiments can be considered 'universal', *i.e.*, suitable for all systems. Each method has its own advantages and limitations.[176] Eventually, the method should be chosen based on the expected properties of the system under study. Probably, a sequential analysis of experimental data by several methods will be appropriate to obtain comprehensive and correct information on the system.

IV. Quantitative interpretation of self-diffusion coefficients

Up to this point, the emphasis was placed on how to correctly (*i.e.*, with minimum errors) measure the SDC. However, a correct interpretation of experimental parameters is at least equally important because, in spite of

¶ The Levenberg – Marquardt method is usually basic to most software packages for processing of DOSY NMR spectra.

† The distinctive features of the DECRA method are as follows: the number of points in the diffusion decay should be even and the PFG amplitude should increase as a quadratic function.[172, 173]

apparent evidence of correlation between the SDC and geometric parameters, there are some aspects which cannot be ignored; otherwise, senseless conclusions can be drawn.

In principle, the interpretation can conditionally be divided into quantitative and qualitative analysis.

Often, SDC measurements mean evaluation of the mobility of the whole molecular species. For instance, if one should answer the question whether does complexation occur in a host–guest system, sometimes it is sufficient to analyze the changes in the SDC of the guest molecules (small molecules characterized by a high SDC) upon addition of host molecules (large molecules characterized by a low SDC) to the solution. If the SDC of the guest molecules decreases and becomes close to that of the host molecules, these types of molecules are bound and eventually move in solution as a single unit. In other words, a strong intermolecular complex is formed in the system.

If one should know the stoichiometry of the complex, the complexation constant, *etc*., a simple evaluation of SDC is insufficient. In this case, analysis of absolute values is required. An intuitively understandable correlation between the SDC and the spatial dimensions of the species under study makes the idea of exact estimation of physical parameters (size, mass) of the species from its SDC attractive. This makes it possible to assess the structure, packing, *etc*. This information became very important recently, when there has been a trend in chemistry of supramolecular systems towards the design of nanoscale molecular ensembles with predetermined properties following the 'bottom–up' approach (an ensemble with a specified structure is assembled from elementary molecular fragments).

At the same time, even if all instrumental sources of errors are eliminated or at least correctly included and the SDC values were corrected, calculations of physical parameters of the system under study from its SDC value is a nontrivial task.

1. Correlation between the self-diffusion coefficients and properties of molecular systems

If the SDC of molecules in solutions are evaluated in the approximation of diffusion of a solid spherical particle in isotropic continuous medium, the Stokes–Einstein equation is used most often

$$D = \frac{kT}{6\pi\eta R_h}, \tag{4}$$

where k is the Boltzmann constant (J K^{-1}), T is absolute temperature (K), η is the viscosity of the solution (N s m^{-2}) and R_h is the hydrodynamic radius (m).

The R_h value includes the radius of the diffusing particle and the thickness of the solvation shell. In studies of self-diffusion of non-spherical particles the parameter R_h is usually interpreted as the average hydrodynamic radius of a solid sphere with the same SDC in the specified solution as the system under study, all other things considered.

At first glance, a correlation between the measured SDC value and the size of the molecular species follows from Eqn (4). To some extent, clearness of this correlation gave an impetus to the development of methods for correct determination of the SDC. Moreover, the simplicity of Eqn (4) is the main reason for a wide use of this relation for evaluation of the size of the system.[177–179] At the same time, one should remember the approximation in which Eqn (4) was derived. Most real molecular systems do not have a spherical shape and real solutions are far from being ideal isotropic media.‡ Clearly, a direct formal application of Eqn (4) for quantitative evaluation may lead to erroneous conclusions.[180]

One can overcome the difficulties mentioned above using two fundamentally different approaches. One of them is based on an improved Stokes–Einstein model, which makes it possible to allow, to some extent, for the difference between the real and an ideal system. The second approach implies an empirical calibration of the 'SDC–parameter' correlation for related systems and subsequent extrapolation of this dependence to the SDC of the system under study in order to estimate the desired parameter. Now we will consider these approaches in more detail.

2. Modification of the Stokes–Einstein equation to describe real systems

From analysis of the prerequisites underlying the Stokes–Einstein model it follows that the smaller the system under study (hydrodynamic radius of the system becomes comparable with the radius of solvent molecules) and/or the greater the deviation of its shape from a sphere (prolate/oblate ellipsoid, long molecular chain) the greater the errors in the size determination using the Stokes–Einstein equation.

A nonideal shape and size of a real molecule can be accounted for by modifying Eqn (4) as follows:[181]

$$D = \frac{kT}{c(r_{sl}, R_h) \times f_s(a,b)\pi\eta R_h}, \tag{5}$$

where $c(r_{sl}, R_h)$ is the coefficient which includes the relative size of the molecules under study (R_h) and the solvent molecules (r_{sl}); and $f_s(a,b)$ is the factor which includes the deviation of the shape of the species under study from the spherical shape.

In the Stokes approximation ($R_h \gg r_{sl}$), the denominator in the right part of Eqn (4) includes a constant equal to 6. Based on the microfriction theory, it was shown[182] that this coefficient decreases as R_h decreases; generally, it depends on the r_{sl}/R_h ratio

$$c(r_{sl}, R_h) = 6\left[\frac{3r_{sl}}{2R_h} + \left(1 + \frac{r_{sl}}{R_h}\right)^{-1}\right]^{-1}.$$

More recently, this expression was refined using the results of semiempirical studies[183]

$$c(r_{sl}, R_h) = 6\left[1 + 0.695\left(\frac{r_{sl}}{R_h}\right)^{2.234}\right]^{-1}.$$

An analysis of these relationships showed that the Stokes–Einstein equation can be used in the classical form (4) only if the radius of the molecules under study is at least five times larger than that of the solvent molecules. For instance, for average-size molecules (radius from 0.3×10^{-9} to 0.6×10^{-9} m) the correction value may vary from 4 to 6. Therefore, the geometric parameters of most

‡ An 'ideal' character of the medium, in particular, implies that experiments are carried out at infinite dilution where the interaction between diffusing species is negligible. This condition is often not met in conventional experiments at finite concentrations.

organic and inorganic molecules estimated using Eqn (4) will include a noticeable error.

The form-factor $f_s(a,b)$ [see Eqn (5)] of a prolate ellipsoid (cigar-shaped molecules) is given by [184, 185]

$$f_s = \sqrt{1-\left(\frac{b}{a}\right)^2}\left[\left(\frac{b}{a}\right)^{2/3}\ln\frac{1+\sqrt{1-(b/a)^2}}{b/a}\right]^{-1},$$

where a and b are the characteristic dimensions of the ellipse.

The form-factor of an oblate ellipsoid (disk-shaped molecules) is given by

$$f_s = \sqrt{\left(\frac{b}{a}\right)^2-1}\left[\left(\frac{b}{a}\right)^{2/3}\mathrm{arctg}\sqrt{\left(\frac{b}{a}\right)^2-1}\right]^{-1}.$$

An analysis of the last two expressions showed that if $a/b > 3$, the error in the results obtained using Eqn (4) will be more than 10%. Also, it is quite probable that the product $c(r_{sl}, R_h) \times f_s(a,b)$ in Eqn (5) will be equal to 6, *i.e.*, Eqn (4) will formally be valid.

Thus, for most practically used molecular species in solutions, Eqn (4) should probably be used with care and only as a first approximation.[186] A more correct analysis requires more complex models that take account of the shape and relative size of the molecule of the compound under study. For instance, in a study of association of planar molecules using this approach it was shown [181] that the shape of dimers is well described by the prolate ellipsoid model (see above). At the same time, the approximations by an oblate ellipsoid and by a sphere led to incorrect results, which made it possible to exclude stacking association.

In spite of clarity of the corrections considered above, this approach is of limited use because the shape of an arbitrary molecular species in solution is very hard to predict. Also, the characteristic R_h value for this species is hard to estimate. As a result, analysis of the measured SDC values requires a number of admissions, which may appear to be sources of errors.

3. Empirical calibration of the SDC/parameter ratio

Thus, the shape of a real molecular species in solution can be very complex and its approximation by a sphere or an ellipsoid may appear to be erroneous. Moreover, it is the volume and mass rather than the characteristic linear dimensions of the system that are often important. An alternative to the quantitative evaluation method described above is based on the search for empirical correlations between particular molecular parameters and the SDC. At first glance, self-diffusion appeared in the Stokes–Einstein model is not related to the mass of the particle; however, a comparison of same-type species showed that in most cases an increase in their hydrodynamic radii (due to an increase in the number of atoms in the molecules) is accompanied by a simultaneous increase in their masses. For polymers, this conclusion is well described by the Flory scaling relation [84, 187–189]

$$R \sim M^{\delta},$$

where R is the linear size of the molecule, M is the molecular mass and δ is the Flory constant.

This expression has a rigorous substantiation within the framework of the fractal theory.[187] Yet another relation valid for such systems has the form

$$R \sim M^{-\alpha}, \quad (6)$$

where α is the parameter which depends on the shape of the species under study.

Thus, having performed measurements for a class of same-type molecular species characterized by similar shapes and character of interactions with solvent molecules and having known masses at specified concentrations, one can derive an empirically parameterized equation relating the SDC of a system to its mass or, *e.g.*, volume. Then, the mass (volume) of a species belonging to the same class can be evaluated from its SDC value with a reasonable accuracy.

This empirical approach proved itself in studies of polymeric systems, *e.g.*, proteins,[190, 191–193] polymers [188, 189, 194] and polysaccharides.[195, 196] It was also successfully used for the determination of the structure of cage compounds [55] and the supramolecular structure of cyclodextrin inclusion complexes,[197] noncovalently bound associates of cyanuric acid and melamine derivatives,[198] a pyrimidine-containing macrocycle [93] and polyoxometallate clusters.[199]

However, it should be noted that the search for an appropriate series of structural analogues of a compound under study is often a complicated task. At the same time, if two similar structures are under identical experimental conditions (ideally, within the same sample), from Eqn (6) it follows that the correlation between the molecular masses M_1, M_2 and the corresponding diffusion coefficients D_1 and D_2 of these structures is given by

$$\frac{D_1}{D_2} = \left(\frac{M_2}{M_1}\right)^{\alpha}, \quad (7)$$

where D_1, M_1 and D_2, M_2 are the SDC and mass of the first and second structure, respectively.

In fact, this interpretation means that the mass (M_2) of the compound under study can be evaluated from its SDC (D_2) and the parameters D_1 and M_1. In one or another form, this idea was used by many researchers who used as references both molecular analogues of the compound under study with the known molecular mass,[55, 195, 196] the solvent molecules,[200, 201] and the chemical shift references.[92]

For instance, studies of highly symmetrical systems often require evaluation of the number of elementary magnetically equivalent (in terms of NMR spectroscopy) fragments in the macrocycle (Fig. 9).[55] Having calibrated the dependence of the SDC on the size (or mass) for a series of structurally similar systems and extrapolated it to the SDC of the compound under study, one can unambiguously determine the structures of such symmetrical systems.[55]

At the same time, it is clear that an arbitrarily chosen compound cannot be used as a reference for calibration of the dependence (7) because the characters of self-diffusion of the molecules of such compounds and the compound under study should be similar.

A method for the determination of the molecular mass using an internal reference was considered in detail.[202] It was shown that the compound to be used as the internal reference should meet the following conditions:

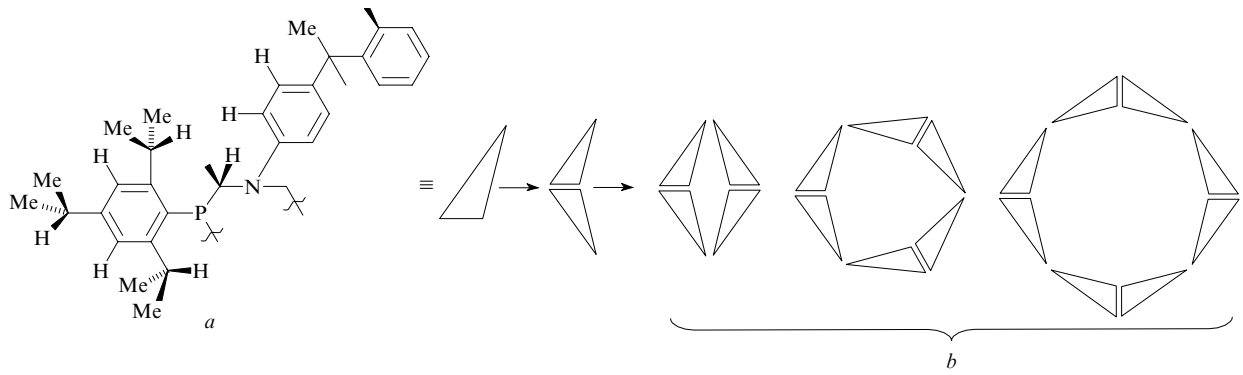


Figure 9. The structure of the repeating unit (*a*) and possible structures of the macrocycle (*b*).

— it should not react and form noncovalent bonds with the compound under study;

— it should be well soluble in the solvent chosen;

— it should have a narrow mass distribution;

— it should have a rather low melting point if one assumes low-temperature experiments;

— its signals in the NMR spectrum should not overlap with the lines of the compound under study; and

— the character of the interaction with the solvent should be the same as that of compound under study.

These requirements are met by hydrocarbons.[202] Correct estimates of the molecular mass can be obtained using 1-tetradecane, cyclooctane and benzene molecules as references. Having thoroughly considered a number of conventional solvents for NMR spectroscopy (toluene, cyclohexane, dichloromethane and chloroform), it was concluded[202] that the addition of the compound under study and three references mentioned above to the solution makes it possible to extend the dependence (6) for these references to the compound under study. Each reference compound can be used individually [see Eqn (7)]. For instance, this approach allowed one to determine the composition of asphaltenes and to assess the size of the constituent molecules.[39]

Thus, to modify the Stokes–Einstein equation, the physical parameters (size, mass, volume) of a molecular species in question can be estimated using the equations for $c(r_{sl}, R_h)$ and $f_s(a,b)$ provided that its shape is *a priori* known. Otherwise, the only way is to construct an empirical dependence (6) for a series of structurally similar compounds including the system in question. If a compound with well-defined parameters (a mass reference or a volume reference) can be added to the sample, the molecular size (mass) of the compound under study can be estimated by simply comparing its SDC with the SDC of this reference compound.

4. Measurements of self-diffusion coefficients in systems with chemical exchange

Yet another source of errors in the interpretation of the measured SDC values appears if the system under study has more than one state corresponding to energy minima on the potential energy surface (*e.g.*, different conformations or associates) and a chemical exchange occurs between these states. The effects of chemical exchange on the chemical shift and SDC values have been well documented.[203–216] Nevertheless, we will briefly outline some aspects of this problem because of its practical importance and an ambiguity due to use of two characteristic time scales in NMR spectroscopy (the chemical shift scale and the SDC scale).

Chemical exchange is a Markovian stochastic process involving transitions of a spin or a group of spins between several states. It is characterized by the rate of chemical exchange. Exchange is called slow on the chemical shift scale if the NMR spectra exhibit resonance signals of different individual spin states (*e.g.*, two conformers). In the case of fast exchange, the spectrum observed is averaged over both states.

The situation on the SDC time scale is different. First, different states of the molecular system are characterized by different geometric parameters. Second, in this case, there is no exchange broadening of spectral lines.[205] Third, the SDC time scale differs from the chemical shift time scale and depends on the experimentally measured diffusion time (parameter Δ, see Fig. 1).[205, 206] Let us give some examples. Generally, a DOSY NMR spectrum can correspond to one of four key regimes of chemical exchange with respect to the rate of the process (Table 2); a wealth of intermediate cases will be left out of consideration. For simplicity, we assume that chemical exchange occurs between two states *A* and *B* only.

Table 2. Chemical exchange regimes on the time scales of chemical shifts and SDC in DOSY NMR spectroscopy.

Regime	Rate of chemical exchange	
	on the chemical shift scale	on the SDC scale
1	slow	slow
2	fast	"
3	slow	fast
4	fast	"

From the standpoint of interpretation, the chemical exchange regime 1 is the simplest. In this case, each set of signals corresponding to different states is characterized by its own SDC value.[40, 41, 63] Moreover, one can make an 'express' estimation of the thermodynamic parameters of chemical exchange. For instance, in the case of formation of pseudocapsules[40] under conditions of the chemical exchange regime 1, the SDC of free guest molecules

(state *A*) appeared to be higher than that of the encapsulated guest molecules (state *B*); this is an additional confirmation of the formation of a molecular ensemble. The relative concentration of the guest molecules in the free and bound states were determined by simply integrating the signals in the diffusion spectrum. Then, the equilibrium constant of encapsulation was calculated.[19,20,40] It should be noted that in this case the integration of the lines in the conventional NMR spectrum would lead to the same results.

The chemical exchange regime 2 is more complicated. In a corresponding system, the states *A* and *B* are characterized by one averaged chemical shift value and different SDC values.§ An example is provided by the chemical exchange of the free and intracellular water molecules.[67] In this case, the thermodynamic parameters cannot be analyzed using the conventional NMR spectrum because of the equal chemical shift values. The only way to determine these thermodynamic parameters is to analyze the DOSY NMR spectrum and to observe individual components.

In the chemical exchange regime 3, the system under study is characterized by different chemical shifts of the states *A* and *B* and by a single SDC value (D_{exp}) determined from the relation [28,205]

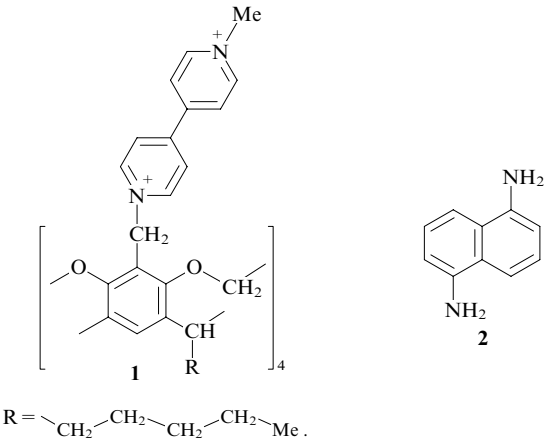
$$D_{exp} = p_A D_A + p_B D_B , \qquad (8)$$

where p_A and p_B are the probabilities for the system to be in the states *A* and *B*, respectively; and D_A and D_B are the SDC of the system in the states *A* and *B*, respectively.

This situation occurs in, *e.g.*, systems where proton exchange between NH groups and free water molecules is possible.[211,213–215] In this case, signals of the NH protons of the molecule under study are observed in the expected low-field region of the ^{1}H NMR spectrum, while the protons that participated in exchange with water molecules contribute to the signal of H_2O and this contribution cannot be separated. As a result, in the DOSY NMR spectrum the SDC value determined for the lines corresponding to the NH protons differs from the SDC determined for the lines of other protons in the molecule, which are not involved in chemical exchange.[211,213–215] A distinctive feature of such systems is that variation of the Δ value specified in the course of experiments leads to observation of the DOSY spectra in which the regime of chemical exchange on the SDC time scale changes from fast to intermediate and then to slow.[213] The SDC value measured for the line of NH protons gradually increases from the value characteristic of the molecule under study to the value characteristic of free water. This allows the rate constant for chemical exchange to be determined.[213,214]

The examples considered above show that in some cases in the interpretation of the DOSY NMR spectra of systems with chemical exchange, not all nuclei in the molecule under study are characterized by the same SDC value. Neglect of this feature will lead to errors in quantification based on analysis of the SDC observed.

§ It is assumed that exchange on the SDC time scale is so slow and the difference between the self-diffusion coefficients is such that mathematical processing of the diffusion decays allows the SDC values of different molecular species to be separated with certainty.



The chemical exchange regime 4 (see Table 2) is the most difficult case. Here, one set of signals is observed on both (SDC and chemical shift) axes. This most often occurs in, *e.g.*, most host–guest systems.[57–62,197] In particular, a study [57] of a mixture of calix[4]resorcinarene (**1**) (host) and naphthalene-1,5-diamine (**2**) (guest) showed that the SDC of compound **2** is higher (0.43×10^{-9} m^2 s^{-1}) than that of compound **1** (0.20×10^{-9} m^2 s^{-1}, Fig. 10 *a*) but smaller than that of individual solution of compound **2**

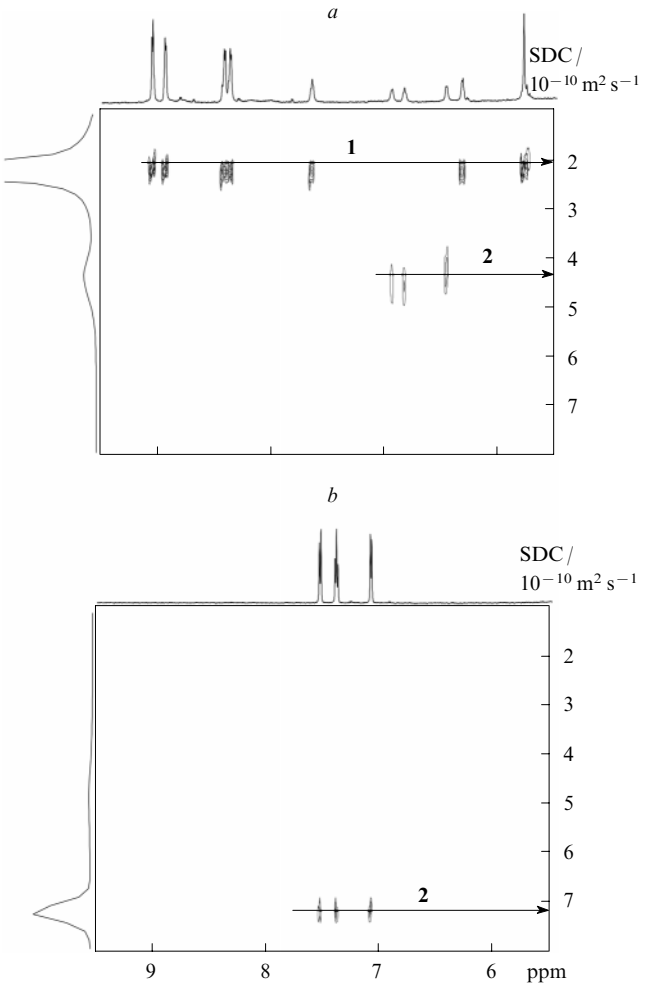


Figure 10. DOSY NMR spectra of systems **1**+**2** (*a*) and **2** (*b*) (^{1}H NMR, 600 MHz, 298 K, in D_2O solution).

(0.72×10^{-9} m^2 s^{-1}, Fig. 10 *b*). In this case, the SDC of the guest molecules is weighted over the free (*A*) and bound (*B*) states involved in fast (on the SDC scale) chemical exchange [see Eqn (8)]. From this one can estimate p_A and p_B using the known SDC values for both states of compound **2** and thus determine the complexation constants.[19, 20, 57, 217]

By definition, the complexation constant in the case of formation of a 1 : 1 complex is given by

$$K = \frac{[HG]}{[H][G]}, \quad (9)$$

where [HG], [H] and [G] are the equilibrium concentrations of the host–guest complex, free host and free guest molecules, respectively, in solution.

Having denoted the initial concentrations of the host and guest molecules in solution $[H]_0$ and $[G]_0$, respectively, one gets

$$[H]_0 = [H] + [HG],$$

$$[G]_0 = [G] + [HG],$$

and the populations of the bound and free states are given by

$$p_B = \frac{[HG]}{[G]_0},$$

$$p_A = \frac{[G]}{[G]_0},$$

respectively. Eventually, expression (9) can be re-written as follows:

$$K = \frac{p_B}{([H]_0 - p_B[G]_0)(1 - p_B)}. \quad (10)$$

Therefore, to determine *K*, it is sufficient to calculate the population of the bound state. In our case (chemical exchange regime 4), taking account of Eqn (8) gives

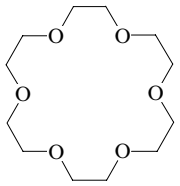
$$p_B = \frac{D_A - D_{exp}}{D_A - D_B}, \quad (11)$$

where D_A and D_B are the SDC of free guest molecules and complexes, respectively.

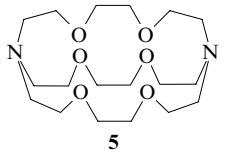
Usually, the host molecules are much larger than the guest ones. Therefore, the SDC of a host–guest complex (D_B) can to a good accuracy be considered equal to the host SDC.¶ Then, the *K* value can be determined with ease by combining Eqns (10) and (11).

Emphasize that this algorithm allows one to calculate the constant *K* from the results of a single DOSY experiment in contrast to traditional NMR experiments based on analysis of the dependence of the chemical shifts of the guest signals upon consecutive increase in the host concentration.[19, 20, 218]

For instance, the ^{1}H chemical shifts in the formation of host–guest complexes in the systems based on $MeN^+H_3Cl^-$ (**3**, guest) and crown ether (**4**) or cryptand (**5**)[219] vary only slightly and cannot be used at all for calculating the complexation constants. However, the approach described above did allow researchers to estimate the complexation constants for the systems **3**+**4** and **3**+**5** and to show that the degree of binding of guest molecules to both hosts in CD_3OD solutions is 2–3 orders of magnitude higher than in water.



4



5

Thus, exchange processes in the system can lead to deviation of the observed SDC from their actual values. Identification of the chemical exchange regimes 1–3 (see Table 2) is relatively simple (owing to the presence of at least one slow process on the NMR time scale). For the regime 4, there are no simple clues and the interpretation may be more complicated and require additional NMR experiments. Therefore, interpretation of the results obtained in the experiments involving SDC measurements should be performed carefully. At the same time, if the occurrence of chemical exchange is established with certainty, one can estimate the energy characteristics of the system.[19, 20, 30, 217–219]

V. Conclusion

The material reported in this review illustrates a considerable progress in the DOSY NMR studies of chemical ensembles, especially supramolecular systems. Improvement of both SDC measurement techniques and methods of interpretation of experimental data and, therefore, the reliability of conclusions is noteworthy. Estimation of diffusion parameters using all advantages of high-resolution NMR spectroscopy opens a unique possibility to determine the size of molecular systems in solutions. In the case of multicomponent ensembles, this allows one to assess their state, character of intermolecular interactions, stability, *etc.*

At the same time, in spite of a rather wide (especially, recent) use of diffusion-ordered NMR spectroscopy, there are still many underlying potential problems of known nature. However, the available equipment is inappropriate to overcome them. This should necessarily be taken into account in the analysis of experimental results, especially with performing their numerical interpretation, in order to avoid erroneous conclusions.

Summing up, note that diffusion-ordered NMR spectroscopy is not a universal tool of studies on supramolecular systems. It does not replace traditional NMR methods based on analysis of the Overhauser effect and chemical shifts, which in some cases provide complementary information. Therefore, a joint analysis of the diffusion, relaxation and NMR spectral parameters could be useful for passage from estimation of empirical parameters of the molecular system (size) to characterization of more subtle features (shape and mutual orientation of components in the system). Interplay different NMR techniques will probably allow one to determine novel subtle structural characteristics of complex supramolecular (multicomponent) systems in liquids.

¶ It should be kept in mind that this approximation does not always 'work' (Ref. 217) and the determination of D_B may require additional experiments.

The review has been written under financial support from the Russian Foundation for Basic Research (Project No. 09-03-00123-a), the Council on Grants at the President of the Russian Federation (under State Programme for Support of Young Researchers and Leading Scientific Schools, Project MK-2622.2009.3). Experimental results were obtained at the NMR Division, Federal Collective Spectro-Analytical Centre for Physicochemical Research on the Structures, Properties and Chemical Composition of Compounds and Materials and at the Federal Centre for Collective Use 'Physicochemical Research on Compounds and Materials'.

References

1. J W Emsley, J Feeney, L H Sutcliffe *High Resolution Nuclear Magnetic Resonance Spectroscopy* (Oxford: Pergamon Press, 1966)
2. J H Noggle, R E Schirmer *The Nuclear Overhauser Effect, Chemical Application* (Oxford: Academic Press, 1971)
3. R R Ernst, G Bodenhausen, A Wokaun *Principles of Nuclear Magnetic Resonance in One and Two Dimensions* (Oxford: Clarendon Press, 1987)
4. D Neuhaus, M P Williamson *The Nuclear Overhauser Effect in Structural and Conformational Analysis* (New York: VCH, 1989)
5. R R Ernst, in *Nobel Lectures, Chemistry 1991 – 1995* (Ed. B G Malmström) (Singapore: World Sci. Publ., 1992) p. 12
6. W R Croasmun, R M K Charlson *Two-Dimensional NMR Spectroscopy. Application for Chemists and Biochemists* (New York: VCH, 1994)
7. Atta-ur-Rahman *One and Two Dimensional NMR Spectroscopy* (Amsterdam: Elsevier, 1989)
8. Yu E Chernysh, V A Volynkin, V T Panyushkin, V I Kondakov, M S Korobov, G S Borodkin *Usp. Khim.* **74** 344 (2005) [*Russ. Chem. Rev.* **74** 317 (2005)]
9. A A Shahkhatuni, A G Shahkhatuni *Usp. Khim.* **71** 1132 (2002) [*Russ. Chem. Rev.* **71** 1005 (2002)]
10. A A Grachev, A G Gerbst, A S Shashkov, N E Nifantiev *Usp. Khim.* **78** 776 (2009) [*Russ. Chem. Rev.* **78** 717 (2009)]
11. L B Krivdin, R Contreras *Annu. Rep. NMR Spectrosc.* **61** 133 (2007)
12. A Balandina, A Kalinin, V Mamedov, B Figadere, Sh Latypov *Magn. Reson. Chem.* **43** 816 (2005)
13. T N Kolokolova, O Yu Savel'ev, N M Sergeev *Zh. Anal. Khim.* **63** 118 (2008) [a]
14. A Balandina, V Mamedov, Sh Latypov *J. Mol. Struct.* **889** 89 (2008)
15. I G Shenderovich, P M Tolstoy, N S Golubev, S N Smirnov, G S Denisov, H-H Limbach *J. Am. Chem. Soc.* **125** 11710 (2003)
16. A V Kozlov, V E Semenov, A S Mikhailov, A V Aganov, M B Smith, V S Reznik, Sh K Latypov *J. Phys. Chem. B* **112** 3259 (2008)
17. Sh Latypov, A Balandina, M Boccalini, A Matteucci, K Usachev, S Chimichi *Eur. J. Org. Chem.* **27** 4640 (2008)
18. D J Blears, S S Danyluk *J. Am. Chem. Soc.* **89** 21 (1967)
19. L Fielding *Tetrahedron* **56** 6151 (2000)
20. K Hirose *J. Inclusion Phenom. Macrocycl. Chem.* **39** 193 (2001)
21. E O Stejskal, J E Tanner *J. Chem. Phys.* **42** 288 (1965)
22. P T Gallaghan *Principles of Nuclear Magnetic Resonance Microscopy* (Oxford: Clarendon Press, 1991)
23. J Karger, H Pfeifer, W Heink *Adv. Magn. Reson.* **12** 1 (1988)
24. R L Haner, T Schleich *Methods Enzymol.* **176** 418 (1989)
25. K F Morris, C S Johnson *J. Am. Chem. Soc.* **114** 3139 (1992)
26. W S Price *Conc. Magn. Reson.* **9** 299 (1997)
27. W S Price *Conc. Magn. Reson.* **10** 197 (1998)
28. C S Johnson Jr *Prog. Nucl. Magn. Reson. Spectrosc.* **34** 203 (1999)
29. B Antalek *Conc. Magn. Reson.* **14** 225 (2002)
30. B Antalek *Conc. Magn. Reson., Part A* **30** 219 (2007)
31. Y Cohen, L Avram, L Frish *Angew. Chem., Int. Ed.* **44** 520 (2005)
32. Y Cohen, L Avram, T Evan-Salem, L Frish, in *Analytical Methods in Supramolecular Chemistry* (Ed. Ch A Schalley) (Weinheim: Wiley, 2007) p. 163
33. A Pastor, E Martinez-Viviente *Coord. Chem. Rev.* **252** 2314 (2008)
34. K Hayamizu, S Tsuzuki, Sh Seki *J. Phys. Chem. A* **112** 12027 (2008)
35. R E Hoffman, H Arzuan, Ch Pemberton, A Aserin, N Garti *J. Magn. Reson.* **194** 295 (2008)
36. C Carrara, St Viel, C Delaurent, F Ziarelli, G Excoffier, St Caldarelli *J. Magn. Reson.* **194** 303 (2008)
37. R Evans, St Haiber, M Nilsson, G A Morris *Anal. Chem.* **81** 4548 (2009)
38. A A Marchione, E F McCord *J. Magn. Reson.* **201** 34 (2009)
39. E Durand, M Clemancey, A-A Quoineaud, J Verstraete, D Espinat, J-M Lancelin *Energy Fuels* **22** 2604 (2008)
40. A Lledo, P Restorp, J Rebek Jr *J. Am. Chem. Soc.* **131** 2440 (2009)
41. A Y Ziganshina, S V Kharlamov, D E Korshin, R K Mukhitova, E Kh Kazakova, Sh K Latypov, V V Yanilkin, A I Konovalov *Tetrahedron Lett.* **49** 5312 (2008)
42. L Avram, Y Cohen *J. Am. Chem. Soc.* **124** 15148 (2002)
43. S V Kharlamov, E P Zhil'tsova, G A Gainanova, L A Kudryavtseva, A P Timosheva, A V Aganov, Sh K Latypov *Kolloid. Zh.* **68** 550 (2006) [b]
44. G A Gainanova, E P Zhil'tsova, L A Kudryavtseva, S V Kharlamov, Sh K Latypov, A P Timosheva, A I Konovalov *Izv. Akad. Nauk, Ser. Khim.* 1359 (2006) [c]
45. A J Dingley, J RMackay, B E Chapman, M B Morris, Ph W Kuchel, B D Hambly, G E King *J. Biomol. NMR* **6** 321 (1995)
46. V V Syakaev, A R Mustafina, J G Elistratova, Sh K Latypov, A I Konovalov *Supramol. Chem.* **20** 453 (2008)
47. E Marotta, F Rastrelli, G Saielli *J. Phys. Chem. B* **112** 16566 (2008)
48. L Zakharova, V Syakaev, M Voronin, V Semenov, F Valeeva, A Ibragimova, A Bilalov, R Giniyatullin, Sh Latypov, V Reznik, A Konovalov *J. Colloid Interf. Sci.* **342** 119 (2010)
49. L Ya Zakharova, V V Syakaev, M A Voronin, F V Valeeva, A R Ibragimova, Y R Ablakova, E Kh Kazakova, Sh K Latypov, A I Konovalov *J. Phys. Chem. C* **113** 6182 (2009)
50. A V Kozlov, V E Semenov, A S Mikhailov, V S Reznik, Sh K Latypov *Tetrahedron Lett.* **49** 6674 (2008)
51. L Galiullina, A Nikolaev, V Semenov, V Reznik, Sh Latypov *Tetrahedron* **62** 7021 (2006)
52. N M Selivanova, O I Gnezdilov, A B Konov, Yu F Zuev, Yu G Galyametdinov *Izv. Akad. Nauk, Ser. Khim.* 495 (2008) [c]
53. Yu F Zuev, R Kh Kurbanov, B Z Idiyatullin,O G Us'yarov *Kolloid. Zh.* **69** 482 (2007) [b]
54. M B M De Azevedo, J B Alderete, A C S Lino, W Loh, A Faljoni-Alario, N Duran *J. Incl. Phenom. Macrocycl. Chem.* **37** 67 (2000)
55. Sh K Latypov, A V Kozlov, E Hey-Hawkins, A S Balueva, A A Karasik, O G Sinyashin *J. Phys. Chem. A* **114** 2588 (2010)
56. A C S Lino, W Loh *J. Incl. Phenom. Macrocycl. Chem.* **36** 267 (2000)
57. S V Kharlamov, A Y Ziganshina, A V Aganov, A I Konovalov, Sh K Latypov *J. Inclusion Phenom. Macrocycl. Chem.* **58** 389 (2007)
58. A Yu Ziganshina, S V Kharlamov, E Kh Kazakova, Sh K Latypov, A I Konovalov *Mendeleev Commun.* **17** 145 (2007)
59. A Gonzalez-Alvarez, I Alfonso, P Diaz, E Garcia-Espana, V Gotor-Fernandez, V Gotor *J. Org. Chem.* **73** 374 (2008)
60. D E Korshin, R R Kashapov, L I Murtazina, R K Mukhitova, S V Kharlamov, Sh K Latypov, I S Ryzhkina, A Y Ziganshina, A I Konovalov *New J. Chem.* **33** 2397 (2009)
61. T Pierro, C Gaeta, F Troisi, P Neri *Tetrahedron Lett.* **50** 350 (2009)
62. S V Kharlamov, A Y Ziganshina, R K Mukhitova, Sh K Latypov, A I Konovalov *Tetrahedron Lett.* **49** 2566 (2008)

63. T S Derrick, L H Lucas, J-L Dimicoli, C K Larive *Magn. Reson. Chem.* **40** S98 (2002)
64. I P Beletskaya, V P Ananikov *Eur. J. Org. Chem.* 3431 (2007)
65. V P Ananikov, I P Beletskaya *Ros. Nanotekhnol.* **4** 56 (2009) [d]
66. V P Ananikov, I P Beletskaya *Izv. Akad. Nauk, Ser. Khim.* 740 (2008) [c]
67. I nslund, D Topgaard *J. Magn. Reson.* **201** 250 (2009)
68. E D Rodrigues, D B Silva, D C R Oliveirac, G V J Silva *Magn. Reson. Chem.* **47** 1095 (2009)
69. S Trefi, V Gilard, St Balayssac, M Malet-Martino, R Martino *Magn. Reson. Chem.* **47** S163 (2009)
70. P Occhipinti, P C Griffiths *Adv. Drug Deliv. Rev.* **60** 1570 (2008)
71. R Marega, V Aroulmoji, F Dinon, L Vaccari, S Giordani, A Bianco, E Murano, M Prato *J. Am. Chem. Soc.* **131** 9086 (2009)
72. W E Maas, F H Laukien, D G Cory *J. Am. Chem. Soc.* **118** 13085 (1996)
73. J Chin, A Chen, M J Shapiro *Magn. Reson. Chem.* **38** 782 (2000)
74. B Sitter, T F Bathen, M-B Tessem, I S Gribbestad *Prog. Nucl. Magn. Reson. Spectrosc.* **54** 239 (2009)
75. O M Rooney, J Troke, J K Nicholson, J L Griffin *Magn. Reson. Med.* **50** 925 (2003)
76. P Weybright, K Millis, N Campbell, D G Cory, S Singer *Magn. Reson. Med.* **39** 337 (1998)
77. Y Perez, H Lahrech, M E Cabanas, R Barnadas, M Sabes, C Remy, C Arus *Cancer Res.* **62** 5672 (2002)
78. H C Gaede, K Gawrisch *Biophys. J.* **85** 1734 (2003)
79. O Wattraint, C Sarazin *Biochim. Biophys. Acta: Biomembr.* **1713** 65 (2005)
80. H C Gaede, K Gawrisch *Magn. Reson. Chem.* **42** 115 (2004)
81. E E Romanova, F Grinberg, A Pampel, J Kärger, D Freude *J. Magn. Reson.* **196** 110 (2009)
82. L Shintu, S Caldarelli *J. Agric. Food Chem.* **54** 4148 (2006)
83. E L Hahn *Phys. Rev.* **80** 580 (1950)
84. A I Maklakov, V D Skirda, N F Fatkullin *Samodiffuziya v Rastvorakh i Rasplavakh Polimerov* (Self-diffusion in Polymer Solutions and Melts) (Kazan: Kazan University, 1987)
85. A R Mutina, V D Skirda *J. Magn. Reson.* **188** 122 (2007)
86. T L James, G G McDonald *J. Magn. Reson.* **11** 58 (1973)
87. P Stilbs, M E Moseley, B Lindman *J. Magn. Reson.* **40** 401 (1980)
88. B Lindman, P Stilbs, M E Moseley *J. Colloid Interf. Sci.* **83** 569 (1981)
89. P Stilbs *Prog. Nucl. Magn. Reson. Spectrosc.* **19** 1 (1987)
90. T Parella *Magn. Reson. Chem.* **36** 467 (1998)
91. M Holz, X Mao, D Seiferling, A Sacco *J. Chem. Phys.* **104** 669 (1996)
92. E J Cabrita, St Berger *Magn. Reson. Chem.* **39** 142 (2001)
93. L Ya Zakharova, V E Semenov, M A Voronin, F G Valeeva, A R Ibragimova, R Kh Giniatullin, A V Chernova, S V Kharlamov, L A Kudryavtseva, Sh K Latypov, V S Reznik, A I Konovalov *J. Phys. Chem. B* **111** 14152 (2007)
94. A J Simpson *Magn. Reson. Chem.* **40** S72 (2002)
95. K Chari, B Antalek, J Minter *Phys. Rev. Lett.* **74** 3624 (1995)
96. S J Doran, M Decorps *J. Magn. Reson. A* **117** 311 (1995)
97. N M Loening, J Keeler, G A Morris *J. Magn. Reson.* **153** 103 (2001)
98. M D Pelta, G A Morris, M J Stchedroff, St J Hammond *Magn. Reson. Chem.* **40** S147 (2002)
99. M J Thrippleton, N M Loening, J Keeler *Magn. Reson. Chem.* **41** 441 (2003)
100. Y Shrot, L Frydman *J. Magn. Reson.* **195** 226 (2008)
101. R J Ordidge, I D Cresshull *J. Magn. Reson.* **69** 151 (1986)
102. G A Morris *J. Magn. Reson.* **80** 547 (1988)
103. P Damberg, J Jarvet, A Graslund *J. Magn. Reson.* **148** 343 (2001)
104. J J V Vaals, A H Bergman *J. Magn. Reson.* **90** 52 (1990)
105. M A Morich, D A Lampman, W R Dannels, F T D Goldie *IEEE Trans. Med. Imag.* **7** 247 (1988)
106. P D Majors, J L Blackley, S A Altobelli, A Caprihan, E Fukushima *J. Magn. Reson.* **87** 548 (1990)
107. P Jehenson, M Westphal, N Schuff *J. Magn. Reson.* **90** 264 (1990)
108. J Jehenson, A Syrota *Magn. Reson. Med.* **12** 253 (1989)
109. S Crozier, F A Beckey, C D Eccles, J Field, D M Doddrell *J. Magn. Reson. B* **103** 115 (1994)
110. W S Price, P W Kuchel *J. Magn. Reson.* **94** 133 (1991)
111. S J Gibbs, C S Johnson *J. Magn. Reson.* **93** 395 (1991)
112. D Wu, A Chen, C S Johnson *J. Magn. Reson. A* **115** 260 (1995)
113. M D Pelta, H Barjat, G A Morris, A L Davis, St J Hammond *Magn. Reson. Chem.* **36** 706 (1998)
114. G Wider, V Dotsch, K Wuthrich *J. Magn. Reson. A* **108** 255 (1994)
115. H Hu, A J Shaka *J. Magn. Reson.* **136** 54 (1999)
116. G A Morris, in *Encyclopedia of Nuclear Magnetic Resonance* (Eds D M Grant, R K Harris) (Chichester: Wiley, 2002) p. 35
117. P Hodge, P Monvisade, G A Morris, I Preece *Chem. Commun.* 239 (2001)
118. B Håkansson, B Jönsson, P Linse, O Söderman *J. Magn. Reson.* **124** 343 (1997)
119. M A Connell, P J Bowyer, P A Bone, A L Davis, A G Swanson, M Nilsson, G A Morris *J. Magn. Reson.* **198** 121 (2009)
120. M Holz, H Weingartner *J. Magn. Reson.* **92** 115 (1991)
121. J S Murday, R M Cotts *Z. Naturforsch. A* **26** 85 (1971)
122. A F Collings, R Mills *J. Chem. Soc., Faraday Trans.* **66** 2761 (1970)
123. H Weingartner *Z. Phys. Chem.* **132** 129 (1982)
124. R Mills *J. Phys. Chem.* **77** 685 (1973)
125. M Holz, R Haselmeier, R K Mazitov, H Weingartner *J. Am. Chem. Soc.* **116** 801 (1994)
126. R Mills, V V M Lobo *Self-diffusion in Electrolyte Solutions* (Amsterdam: Elsevier, 1989)
127. N N Yadav, A M Torres, W S Price *J. Magn. Reson.* **194** 25 (2008)
128. F D Doty, G Entzminger, Y A Yang *Conc. Magn. Reson.* **10** 133 (1998)
129. H Kato, T Saito, M Nabeshima, K Shimada, S Kinugasa *J. Magn. Reson.* **180** 266 (2006)
130. M L Tillett, L Y Lian, T J Norwood *J. Magn. Reson.* **133** 379 (1998)
131. S M Zhang *J. Am. Chem. Soc.* **128** 4974 (2006)
132. S M Zhang *Chem. Phys. Chem.* **8** 635 (2007)
133. S V Kharlamov, Candidate Thesis in Chemical Sciences, Institute of Organic and Physical Chemistry, Kazan Research Centre of the Russian Academy of Sciences, Kazan, 2008
134. St Viel, F Ziarelli, G Pages, C Carrara, St Caldarelli *J. Magn. Reson.* **190** 113 (2008)
135. K Hayamizu, W S Price *J. Magn. Reson.* **167** 328 (2004)
136. I V Koptyug, R Z Sagdeev *Usp. Khim.* **71** 672 (2002) [*Russ. Chem. Rev.* **71** 593 (2002)]
137. W J Goux, L A Verkruyse, S J Salter *J. Magn. Reson.* **88** 609 (1990)
138. X-A Mau, O Kohlmann *J. Magn. Reson.* **150** 35 (2001)
139. M Nilsson, G A Morris *J. Magn. Reson.* **177** 203 (2005)
140. K I Momot, Ph W Kuchel *J. Magn. Reson.* **174** 229 (2005)
141. Ya I Frenkel' *Kineticheskaya Teoriya Zhidkostei* (Kinetic Theory of Liquids) (Moscow: Academy of Sciences of the USSR,1945)
142. E Martinez-Viviente, P S Pregosin *Helv. Chim. Acta* **86** 2364 (2003)
143. A Jerschow, N Muller *J. Magn. Reson.* **125** 372 (1997)
144. A Jerschow, N Muller *J. Magn. Reson.* **132** 13 (1998)
145. G H Sørland, J G Seland, J Krane, H K Anthonsen *J. Magn. Reson.* **142** 323 (2000)
146. A Pampel, M Fernandez, D Freude, J Kärger *Chem. Phys. Lett.* **407** 53 (2005)
147. J E Tanner *J. Chem. Phys.* **52** 2523 (1970)
148. H Zhang, R Kerssebaum, R M Gschwinda *Magn. Reson. Chem.* **47** 568 (2009)
149. V Y Orekhov, D M Korzhnev, K V Pervushin, E Hoffman, A S Arseniev *J. Biomol. Struct. Dynam.* **17** 157 (1999)

150. W-Y Choy, F A A Mulder, K A Crowhurst, D R Muhandiram, I S Millett, S Doniach, J D Forman-Kay, L E Kay *J. Mol. Biol.* **316** 101 (2002)
151. F Ferrage, M Zoonens, D E Warschawski, J-L Popot, G Bodenhausen *J. Am. Chem. Soc.* **125** 2541 (2003)
152. M Carravetta, M H Levitt *J. Chem. Phys.* **122** 214505 (2005)
153. S Cavadini, J Dittmer, S Antonijevic, G Bodenhausen *J. Am. Chem. Soc.* **127** 15744 (2005)
154. L J C Peschier, J A Bouwstra, J Bleyser, H E Junginger, J C Leyte *J. Magn. Reson. B* **110** 150 (1996)
155. S V Dvinskikh, I Furó *J. Magn. Reson.* **146** 283 (2000)
156. A Chen, M Shapiro *J. Am. Chem. Soc.* **121** 5338 (1999)
157. M Nilsson, M A Connell, A L Davis, G A Morris *Anal. Chem.* **78** 3040 (2006)
158. A N Kolmogorov *Usp. Mat. Nauk* **1** 57 (1946)
159. P R Bevington *Data Reduction and Error Analysis for the Physical Sciences* (New York: McGraw-Hill, 1969)
160. S W Provencher *J. Chem. Phys.* **64** 2772 (1976)
161. S W Provencher *Biophys. J.* **16** 27 (1976)
162. S W Provencher, R H Vogel, in *Numerical Treatment of Inverse Problems in Differential and Integral Equations* (Eds P Deuflhard, E Hairer) (Boston: Birkhauser, 1983) p. 304
163. Y Zhu, R B Gregory *Nucl. Instrum Methods. A* **284** 443 (1989)
164. K F Morris, C S Johnson Jr *J. Am. Chem. Soc.* **115** 4291 (1993)
165. R S Stock, W H Ray *J. Polym. Sci.: Polym. Phys. Ed.* **23** 1393 (1985)
166. J Jakes *Czech. J. Phys. B* **38** 1305 (1988)
167. K F Morris, C S Johnson Jr, T C Wong *J. Phys. Chem.* **98** 603 (1994)
168. M A Delsuc, T E Malliavin *Anal. Chem.* **70** 2146 (1998)
169. T E Malliavin, V Louis, M A Delsuc *J. Chim. Phys. Phys. Chim. Biol.* **95** 178 (1998)
170. M Kubista *Chemom. Intell. Lab. Syst.* **7** 273 (1990)
171. D Schulze, P Stilbs *J. Magn. Reson. A* **105** 54 (1993)
172. B Antalek, W Windig *J. Am. Chem. Soc.* **118** 10331 (1996)
173. W Windig, B Antalek *Chemom. Intell. Lab. Syst.* **37** 241 (1997)
174. L C Van Gorkom, T M Hancewicz *J. Magn. Reson.* **130** 125 (1998)
175. P Stilbs, K Paulsen, P C Griffiths *J. Phys. Chem.* **100** 8180 (1996)
176. R Huo, R Wehrens, J V Duynhoven, L M C Buydens *Anal. Chim. Acta* **490** 231 (2003)
177. R Xue, Sh Wang, H Qi, Y Song, Ch Wang, F Li *Biochim. Biophys. Acta* **1778** 1444 (2008)
178. A H Daranas, J J Fernandez, E Q Morales, M Norte, J A Gaven *J. Med. Chem.* **47** 10 (2004)
179. H Pei, M W Germann, S A Allison *J. Phys. Chem. B* **113** 9326 (2009)
180. M Sharma, S Yashonath *J. Phys. Chem. B* **110** 17207 (2006)
181. A Macchioni, G Ciancaleoni, C Zuccaccia, D Zuccaccia *Chem. Soc. Rev.* **37** 479 (2008)
182. A Gierer, K Z Wirtz *Z. Naturforsch., A* **8** 522 (1953)
183. H-C Chen, S-H Chen *J. Phys. Chem.* **88** 5118 (1984)
184. F Perrin *J. Phys. Radium.* **7** 1 (1936)
185. G Li, J X Tang *Phys. Rev. E* **69** 061921 (2004)
186. L Allouche, A Marquis, J-M Lehn *Chem. – Eur. J.* **12** 7520 (2006)
187. P Flory *Princinples of Polymer Chemistry* (New York: Cornell University Press, 1978)
188. A Jerschow, N Müller *Macromolecules* **31** 6573 (1998)
189. B Håkansson, M Nyden, O Söderman *Colloid Polym. Sci.* **278** 399 (2000)
190. J Danielsson, J Jarvet, P Damberg, A Graslund *Magn. Reson. Chem.* **40** S89 (2002)
191. Sh Yao, G J Howlett, R S Norton *J. Biomol. NMR* **16** 109 (2000)
192. D K Wilkins, S B Grimshaw, V Receveur, C M Dobson, J A Jones, L J Smith *Biochemistry* **38** 16424 (1999)
193. I V Nesmelova, V D Skirda, V D Fedotov *Biopolymers* **63** 132 (2002)
194. S Auge, P-O Schmit, Ch A Crutchfield, M T Islam, D J Harris, E Durand, M Clemancey, A-A Quoineaud, J-M Lancelin, Y Prigent, F Taulelle, M-A Delsuc *J. Phys. Chem. B* **113** 1914 (2009)
195. St Viel, D Capitani, L Mannina, A Segre *Biomacromolecules* **4** 1843 (2003)
196. P Groves, M O Rasmussen, M D Molero, E Samain, F J Canada, H Driguez, J Jimenez-Barbero *Glycobiology* **14** 451 (2004)
197. K S Cameron, L Fielding *Magn. Reson. Chem.* **40** S106 (2002)
198. P Timmerman, J-L Weidmann, K A Jolliffe, L J Prins, D N Reinhoudt, S Shinkai, L Frish, Y Cohen *J. Chem. Soc., Perkin Trans. 2* 2077 (2000)
199. S Floquet, S Brun, J-F Lemonnier, M Henry, M-A Delsuc, Y Prigent, E Cadot, F Taulelle *J. Am. Chem. Soc.* **131** 17254 (2009)
200. C A Crutchfield, D J Harris *Magn. Reson. Chem.* **45** 463 (2007)
201. C A Crutchfield, D J Harris *J. Magn. Reson.* **185** 179 (2007)
202. D Li, G Kagan, R Hopson, P G Williard *J. Am. Chem. Soc.* **131** 5627 (2009)
203. C S Johnson Jr, in *Advances in Magnetic Resonance* Vol. 1 (Ed. J S Waugh) (New York: Academic Press, 1965) p. 33.
204. S W Englander, L Mayne *Annu. Rev. Biophys. Biomol. Struct.* **21** 243 (1992)
205. C S Johnson Jr *J. Magn. Reson. A* **102** 214 (1993)
206. C T H Moonen, P V Gelderen, G W Vuister, P C M V Zijl *J. Magn. Reson.* **97** 419 (1992)
207. G Wagner, K Wuthrich *J. Mol. Biol.* **160** 343 (1982)
208. M Delepierre, C M Dobson, M Karplus, F M Poulsen, D J States, R E Wedin *J. Mol. Biol.* **197** 111 (1987)
209. H Roder, G A Elöve, S W Englander *Nature (London)* **335** 700 (1988)
210. S Grzesiek, A Bax *J. Biomol. NMR* **3** 627 (1993)
211. E J Cabrita, S Berger, P Brauer, J Kärger *J. Magn. Reson.* **157** 124 (2002)
212. A Bockmann, E Guittet *FEBS Lett.* **418** 127 (1997)
213. E J Cabrita, St Berger *Magn. Reson. Chem.* **40** S122 (2002)
214. P Thureau, B Ancian, St Viel, A Thevand *Chem. Commun.* 200 (2006)
215. T Brand, E J Cabrita, G A Morris, R Gunther, H-J Hofmann, St Berger *J. Magn. Reson.* **187** 97 (2007)
216. S Leclerc, L Guendouz, A Retournard, D Canet *Conc. Magn. Reson., Part A* **36** 127 (2010)
217. K S Cameron, L Fielding *J. Org. Chem.* **66** 6891 (2001)
218. S Simova, St Berger *J. Inclusion Phenom. Macrocycl. Chem.* **53** 163 (2005)
219. O Mayzel, Y Cohen *J. Chem. Soc., Chem. Commun.* 1901 (1994)

[a] — *J. Anal. Chem. (Engl. Transl.)*
[b] — *Colloid. J. (Engl. Transl.)*
[c] — *Russ. Chem. Bull., Int. Ed. (Engl. Transl.)*
[d] — *Nanotechnol. Russ. (Engl. Transl.)*